

AD-A162 967

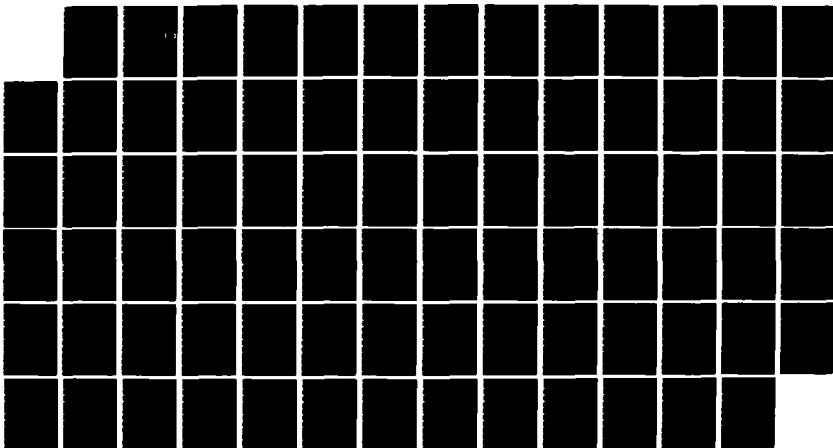
NONLINEAR EARTHQUAKE ANALYSIS OF CONCRETE BUILDING
STRUCTURES(U) ILLINOIS UNIV AT URBANA D P ABRAMS
SEP 85 N00014-83-D-0689

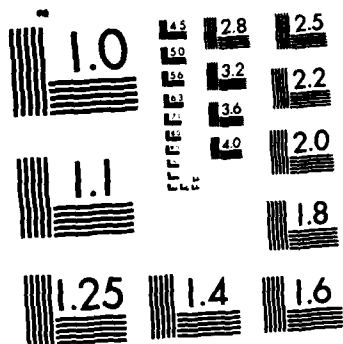
1/1

UNCLASSIFIED

F/G 13/13

NL





MICROCOPY RESOLUTION TEST CHART
NATIONAL BUREAU OF STANDARDS-1963-A

12

N00014-83-D-0689

AD-A162 967

NONLINEAR EARTHQUAKE ANALYSIS
OF CONCRETE BUILDING STRUCTURES

by

DANIEL P. ABRAMS

Associate Professor
University of Illinois at Urbana-Champaign

DTIC
ELECTE
JAN 6 1986
S D

a final report on a study to the

American Society for Engineering Education
Postdoctoral Fellowship Program

sponsored by the

U.S. Navy
Office of Naval Technology

DTIC FILE COPY

DISTRIBUTION STATEMENT A
Approved for public release
Distribution Unlimited

September 1985

85 12 6 101

Table of Contents

1.0	Introduction.....	Page 2
2.0	Object and Scope of Study.....	3
3.0	Intended Utilization of Analytical Technique.....	3
4.0	Background Information	
4.1	Introductory Remarks.....	4
4.2	Inelastic Behavior of RC Structures.....	4
4.3	Numerical Methods for Computation.....	9
5.0	Description of Computational Technique	
5.1	Introductory Remarks.....	10
5.2	Theoretical Derivation	
5.2.1	Computation of Response for SDOF.....	11
5.2.2	Generalized Formulation of Hysteresis....	14
5.2.3	Earthquake Ground Motions.....	17
5.2.4	Modal Decoupling Procedure.....	20
5.3	Application of Technique	
5.3.1	Introductory Remarks.....	26
5.3.2	Rapid Nonlinear Dynamic Analysis.....	27
5.3.3	Explicit Consideration of Stiffnesses....	30
6.0	Verification and Sample Results	
6.1	Verification of Procedure with Measurements....	30
6.2	Sample Results of Procedure.....	35
7.0	Future Development.....	42
8.0	References.....	43
	Appendix A: Manual for Program Usage.....	45
	Appendix B: Program Listing.....	58
	Appendix C: Earthquake Records.....	67

ACKNOWLEDGMENTS

The study described in this report was done as part of activities of the author during a seven-month fellowship at the Naval Civil Engineering Laboratory at Port Hueneme, California. The fellowship was funded by the Office of Naval Technology and administered by the American Society for Engineering Education. Appreciation is extended to Charles Carter and Paul Nicolas of ASEE, and Stephen Ehret of NCEL, for management of the program.

The writer wishes to thank William Armstrong, Theodore Shugar, Stanley Takahashi, and John Ferritto at NCEL for their interest and support of the work.

Accession For	
NTIS CRA&I	
DTIC TAB	
Unannounced	
Justification	
<i>William Armstrong</i>	
By	
Distribution /	
Availability Codes	
Dist	Availability or Special
A-1	



1.0 Introduction

Proportioning of strength in an earthquake resistant structure is usually based on a linear elastic analysis and a set of equivalent static lateral forces. This design procedure has proven to be reliable on the basis of observed building damage caused by past earthquakes and has been adopted by present building codes (1,2).

The energy dissipated by a structure is enhanced once the elastic limit is exceeded. This fact has been substantiated by experiments of model ten-story structures (3). Larger lateral forces were attracted to test structures with walls that were designed to remain elastic (Fig. 1.1) than to structures that could dissipate energy through nonlinear effects. Lateral deflections of each structure were similar (Fig. 1.2) indicating that serviceability was not influenced significantly by inelastic action.

The code approach accounts for inelastic behavior implicitly by prescribing lower forces than what would be necessary on the basis of linear behavior alone. However, the limit of the nonlinear deformation, or the nature of the inelastic force-deflection relation is not considered. Furthermore, the complex interaction of the softening structure and the frequency content, sequence and intensity of the ground motion is not represented. Structures with symmetrical and asymmetrical resistances are considered to behave equally. Because the approximate static procedure must lead to a conservative design, it is likely that a more accurate depiction of the inelastic response history would result in safer designs with lower costs. This would apply to both construction of new structures and rehabilitation of existing ones.

It is now possible to replace approximate design techniques with exact solutions based on simple rules of mechanics. Using a personal computer, inelastic response histories can be computed in a matter of seconds with a similar effort as former "hand" calculations. Simplifying assumptions do not need to be made. An explicit analysis of the response history can indicate energy dissipation characteristics of a particular hysteretic oscillator more precisely than past approximate methods. Furthermore, the analysis can estimate the number of cycles at a particular level of inelastic deformation that the structure should incur. This is an important parameter that has previously not been considered for design, but is vital to the prediction of damage accumulation.

Presently, inelastic design of concrete structures subjected to load reversals is an art much like design of continuous structures subjected to gravity loadings was in the earlier part of the century. Inelastic stiffness characteristics of concrete components have been shown through experiments to be influenced by parameters not previously considered for analysis of structures subjected to monotonically increasing forces. Hysteretic behavior of members and connections have been shown to be dependent on opening and closure of flexural and shear cracks, bond-slip mechanisms, softening of

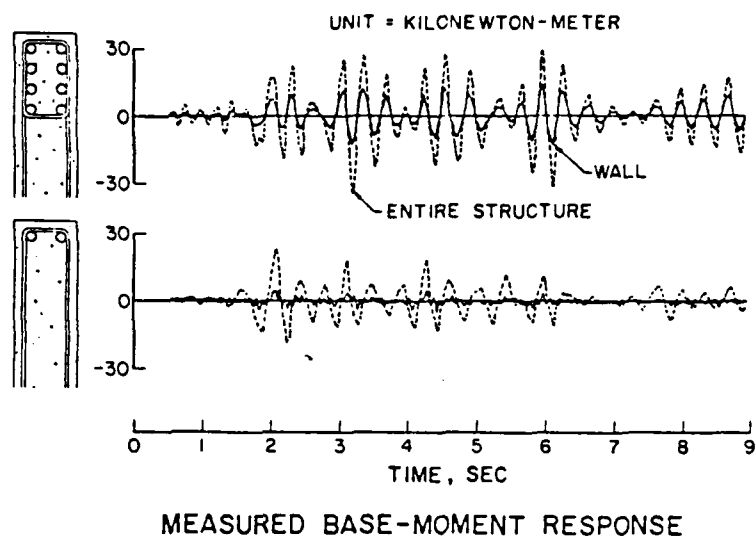


Fig. 1.1 Comparison of Lateral Forces for Elastic and Inelastic Designs

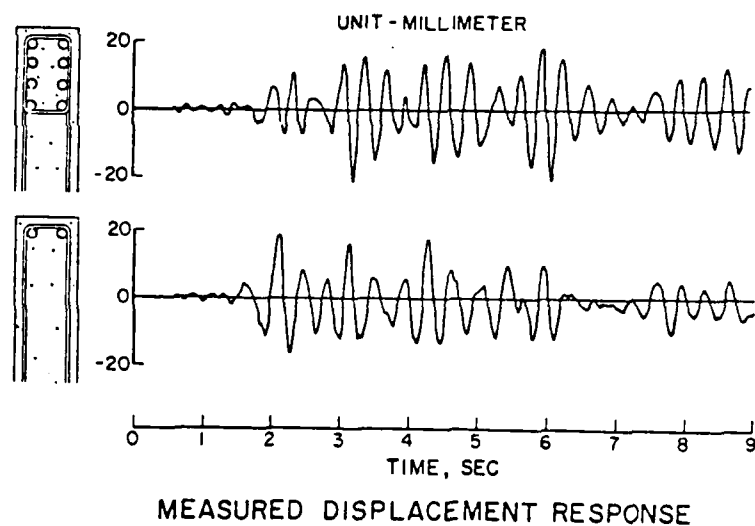


Fig. 1.2 Comparison of Lateral Deflections for Elastic and Inelastic Designs

reinforcement, and inelasticity of concrete in compression. Because of the complexity of inelastic behavior and the uncertain sequence of ground excitations, several analyses need to be done so that an engineer may develop the judgement needed to implement a particular design. A simple tool needs to be developed for these analyses.

2.0 Object and Scope

The purpose of study described in this report is to develop an analytical technique that considers explicitly both the history of the ground motion, and the nonlinear hysteretic behavior of the structure. The technique is developed using nonlinear resistance characteristics of reinforced concrete structures, however, the basis of the method is applicable to any type of building structure.

The method is verified by correlating calculated response with that measured of model structures subjected to simulated earthquake motions.

3.0 Intended Utilization of Analytical Technique

The analytical technique is intended to augment present methods used for estimating dynamic response of building structures, and assessing their vulnerability to moderate or strong earthquake motions. Input for the analysis may be based on either a rapid and approximate identification of system properties, or a more lengthy conventional static linear analysis. Output from the analysis includes response histories of the input motion, acceleration at the top level, maximum interstory lateral drift, and the hysteretic relation between base shear and top-level deflection.

4.0 Background Information

4.1 Introductory Remarks

To help understand why and how nonlinear response should be considered for design or analysis of a structure, short compilations follow on (a) the nature of inelastic behavior for reinforced concrete structures, and (b) present techniques used for computation of response.

4.2 Inelastic Behavior of Reinforced Concrete Structures

Numerous experimental studies have investigated the nonlinear behavior of structural members and connections under repeated and reversed loadings. A report compiled by the Applied Technology Council provides a comprehensive summary of test results (4). A future publication of the American Concrete Institute (5) will also provide a summary of experimental results for wall elements, beams, columns, and beam-column joints subjected to loading reversals.

Experimental tests have shown that behavior of reinforced concrete members and connections under load reversals are not governed solely by constitutive properties of materials. Substantial deflections may be a result of opening and closing of flexural or shear cracks, and slippage of reinforcing bars relative to concrete. Most tests of concrete components have shown that after a few large-amplitude cycles, specimens respond with a marked reduction in resistance upon reversal of the load (Fig. 4.1). After deflections are reversed an amount "a" or "b", specimens stiffen as cracks close. Because of bar slippage and crack closure in the load-reversal range, and reductions in loading stiffnesses, " k_1 " and " k_2 ", strengths are reached at deflections which are much larger than would occur under static acyclic forces. Most specimens tested deformed very large amounts without suffering a significant loss of strength, however, energy dissipation characteristics were poor for those specimens that had incurred substantial slippage in the load-reversal region.

Tests have shown that inelastic behavior is quite dependent on the number of large-amplitude cycles. Tensile strains in the reinforcement are seldom balanced with equal compressive strains for opposite directions of loading because of the added resistance of concrete to aid steel when in compression. If the reinforcement yields while in tension, strains will accumulate with each large-amplitude cycle of deformation. After a sufficient number of cycles, the width of flexural cracks will enlarge which will result in marked differences in stiffness and strength characteristics.

In addition to unequal tension-compression straining of reinforcement, sections and members are subjected to unequal inelastic curvatures and rotations for each direction of loading. Like the strains, these deformations

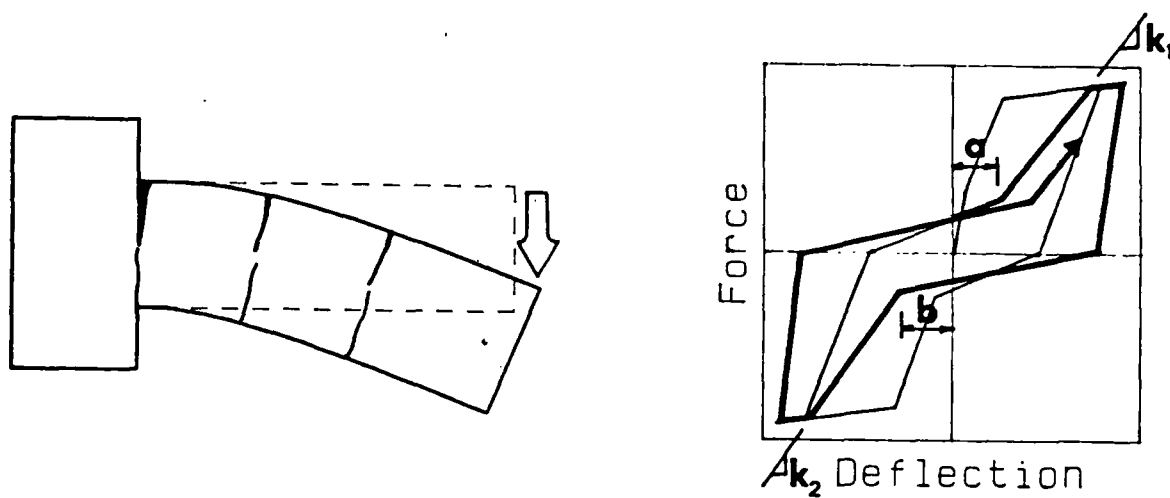


Fig. 4.1 General Hysteretic Relation for Reinforced Concrete Member

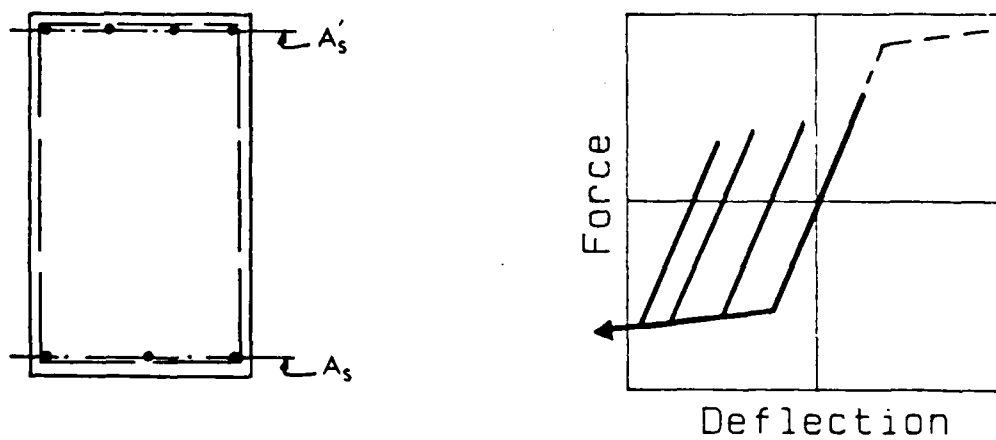


Fig. 4.2 Accumulation Effects for Asymmetrical Strengths

accumulate with each large-amplitude cycle. A simple example helps to illustrate this phenomena. Design of negative reinforcement entails an assumption regarding the amount of maximum gravity loading which will probably be present during an earthquake. In actuality, it is conceivable that a lesser amount of gravity loading may be present than assumed for design. In this case, the top steel will not strain as much as the bottom steel, and perhaps may not yield at all (Fig. 4.2). This results in inelastic rotation which accumulates for each large-amplitude cycle, resulting in large crack widths and a possible reduction in shear capacity.

Similar illustrations can be made for other typical cases where the proportioning of resistance is not in absolute accordance with actual phenomena. Conservative design assumptions with respect to the effective flange width of T-beams (Fig. 4.3) may result in asymmetrical straining of top and bottom reinforcement, and thus, an accumulation of tensile plastic strains in the bottom reinforcement. This phenomena is augmented by asymmetrical elastic stiffnesses which are a result of differences in flange effectiveness when in tension or compression. For equal sways of the structure in each direction, the bottom reinforcement may yield whereas the top would not.

Tests of beam-column joints have shown that inelastic behavior is sensitive to bond mechanisms under repeated and reversed loadings. Free-body diagrams (Fig 4.4) illustrate the difference in bond demands for beam reinforcement in exterior and interior-joint specimens. For interior-joint specimens (Fig. 4.5a), bond strength for beam reinforcement was lost across the width of the column member which eliminated the effectiveness of the bars to resist compression. Upon reversal of the load, specimen stiffness reduced to zero because reinforcement was not effective to resist closure of the previously opened flexural crack. After the crack closed, the specimen stiffened until the tensile reinforcement reached its proportional limit. However, because of the large amount of slippage within the load-reversal region, strengths were reached at very large deflections. Specimens withstood very large inelastic deflections (in excess of 4% of the story height), however, they did not resist a substantial amount of energy. Demand for bond strength was less for bars in the exterior-joint specimens (Fig. 4.5b). The severe stiffness reduction upon reversal of the load did not occur, and the specimen was able to resist more energy.

Knowledge of the inelastic behavior of members is necessary, but not sufficient, to understand the behavior of a structural system. A large-scale test of a seven-story concrete building (6) has shown that a planar representation of lateral-load resisting elements may not suffice to depict the strength or stiffness characteristics of an overall structure. For this particular frame-wall structure, uplift of a rocking shear wall relative to adjacent frames resulted in substantial axial compressive forces in the wall. This increased the strength of the structure, but decreased the anticipated capacity of the structure to deform inelastically.

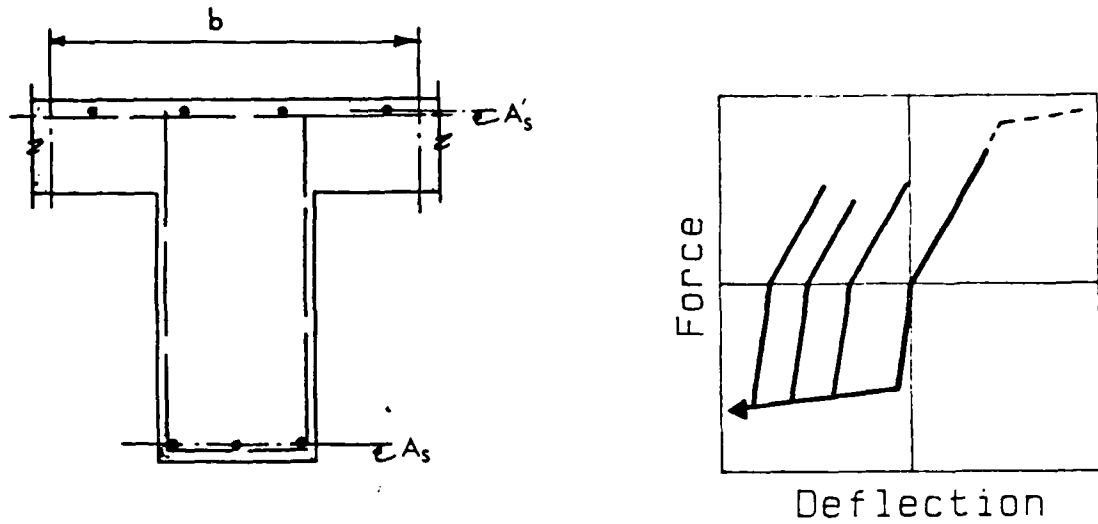


Fig. 4.3 Accumulation Effects for Asymmetrical Strengths and Stiffnesses

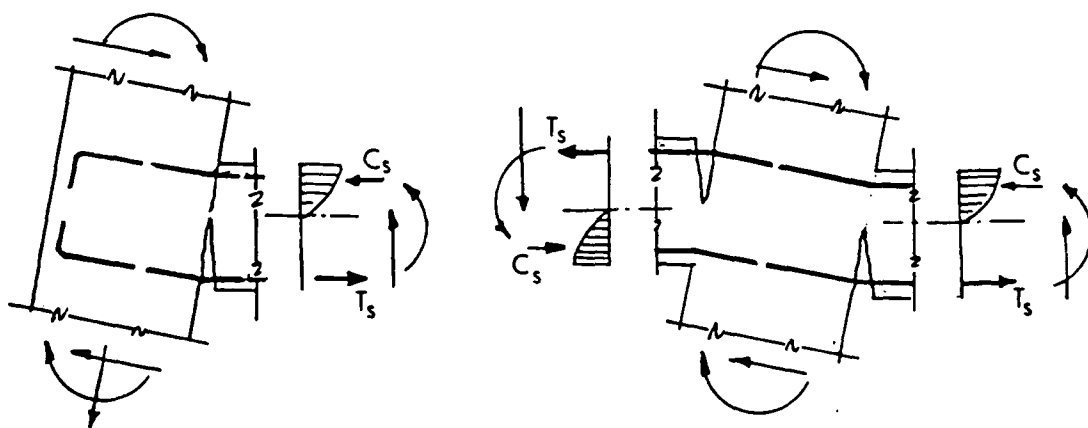


Fig. 4.4 Free-Body Diagrams for Beam-Column Joints

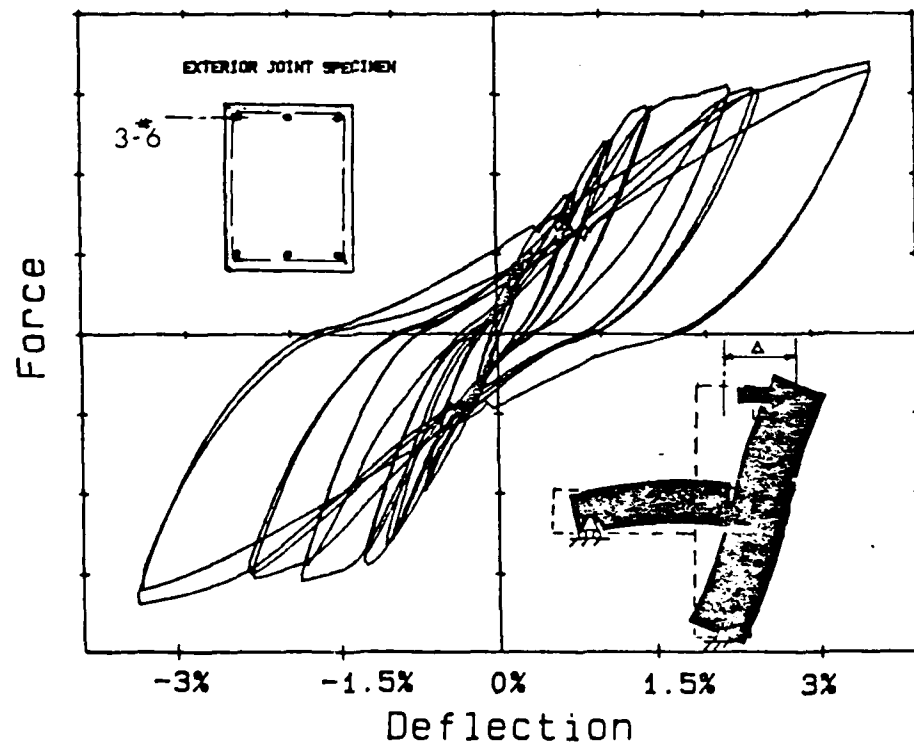
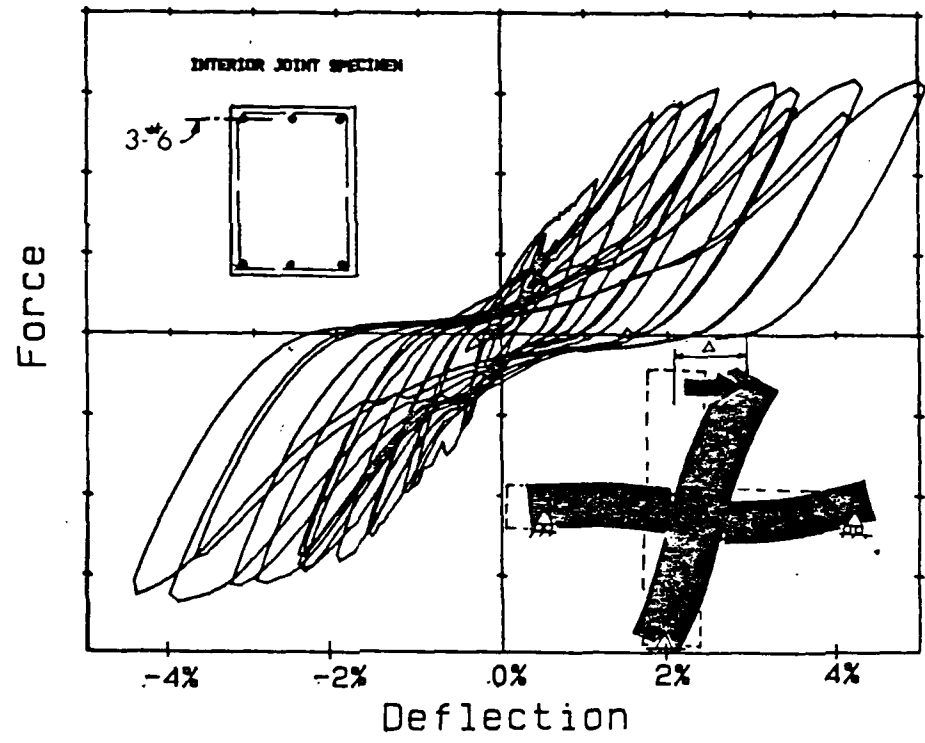


Fig. 4.5 Measured Force-Deflection Curves for Interior and Exterior Beam-Column Joints

These few examples show that modeling of inelastic behavior of reinforced concrete structures still remains an art. A reasonable depiction of nonlinear behavior for an actual structure requires a substantial amount of judgement, and is quite subjective. Several analyses should be done representing bounds of expected behavior.

4.3 Numerical Methods for Computation of Nonlinear Response

The exact procedure for determining the response of an oscillator subjected to an earthquake, or any dynamic loading, is to integrate the equation of motion numerically for several instants in time. For elastic systems, an approach may be used where response due to differential impulses are superimposed at each instant. This approach is commonly known as the Duhamel Integral (7). For nonlinear systems, superposition is not valid, and the equation of motion must be integrated at each instant. If a variation in acceleration across a time step is assumed, then displacement and velocity at the end of the time step can be derived in terms the acceleration at the end of the step. Using the dynamic equilibrium equation, a new acceleration can be derived which should converge to the assumed acceleration after a few number of iterations. This is the method developed by Newmark (8). Either of these two methods requires an explicit description of an earthquake record. The reliance on magnetic tape facilities and the length of the computation has made this procedure inappropriate for hand calculation in the past.

To reduce the amount of computation, response spectra are used to represent maximum response of oscillators with a range of natural frequencies. An engineer, knowing the modal frequencies of a structural system, can estimate amplification of ground accelerations for each mode by simply reading from the spectral-response curve. Frequency characteristics of different ground motions can be studied by comparing their spectra. Response spectra are generated for elastic systems using a numerical integration of the equation of motion for a particular ground motion, however, as mentioned below, they have been adjusted to model nonlinear behavior.

Because future ground motions are unknown or at best probabilistic, an approximate method was developed by Newmark and Hall (9). Rather than use time-step integration, smoothed spectral response curves are constructed on an approximate basis. Amplification of peak ground motions are estimated based on the foundation medium for ranges of constant acceleration, velocity or displacement.

A further sophistication developed by Newmark and Hall (9) was to use the elastic response spectra to represent maximum amplitudes of motion for nonlinear systems. A ductility factor, defined as the ratio of maximum to yield displacements, was used to express relations between kinetic energies of elastic and elasto-plastic systems. In this way, inelastic spectra could be generated directly from elastic spectra. Lai and Biggs (10) found that this approach may give unconservative response estimates for oscillators with 5%

damping. They suggested improvements for the construction of inelastic spectra which are similar to the ones proposed by Riddell and Newmark (11).

Studies (12,13) have been done to examine inelastic spectral response for systems with more realistic, and more complicated, load-deflection relations than the elasto-plastic formulation assumed by Newmark and Hall. Spectral response has been computed by integrating the equation of motion numerically with various hysteresis models. Resistances of the overall structure have been modeled with polylinear, stiffness degrading and softening-hardening formulations. Parameters plotted on spectra have included the strength ratio (provided strength to weight of structure), the number of large-amplitude cycles, and the cyclic accumulated ductility. Because of the complexity with respect to normalizing characteristics of hysteresis models, it is impractical for these spectra to be used in a design context. However, many salient conclusions have resulted. One such conclusion is that an elasto-plastic formulation may be unconservative in predicting response maxima because it results in an upper bound for the energy dissipated by an oscillator.

5.0 Description of Computational Technique

5.1 Introductory Remarks

A simple method of computation needs to be developed which characterizes the hysteretic resistance of the structure and the frequency content, sequence and intensity of the ground motion; and determines the maximum amount of nonlinear deformation, the number of cycles of nonlinear deformation, and an estimate of equivalent static forces for which the structure should be designed. The method should be sufficiently simple and quick so that an engineer may perform several analyses of the structure to identify all possible bounds of behavior for a range of expected ground motions.

With the recent introduction of personal computers, structural engineers are equipped with a utility that they can understand and control. Easy access to a computational device from a desktop has, and shall continue to revolutionize engineering practices. The influence of several parameters may now be studied with the same amount of effort that a single analysis once took. Spectral-response curves may now be replaced with direct computation of response histories from ground motion records. Because of the recursive nature of the computation, the analysis may be done in a matter of seconds on a personal computer. The fact that an oscillator may respond nonlinearly is unimportant to the degree of difficulty.

At present, personal computers are limited in speed and storage capacity for practical computation of response for systems with more than a few degrees of freedom. However, for structures as tall as ten stories, research has shown that this limitation may not be restrictive. Tests of model structures responding within the nonlinear range of response (3) have shown that deflected shapes were nearly constant for all amplitudes of motion. This suggests that it is plausible to represent response with a single coordinate and a known distribution of deflection even though it may behave within the nonlinear range of response. This concept was developed further by Saiidi (14) and served as the basis for the "Q" model. The computational effort reduces substantially to the range of capabilities of a personal computer if this simplifying assumption is made.

On the basis of this theory, mass, stiffness and strength properties of an overall structure may be condensed to a single dynamic degree of freedom. For example, definition of the relation between base shear and top-level displacement would suffice to represent the nonlinear resistance of the structure. The proposed analytical technique which is described in the next section is based on this concept.

5.2 Theoretical Derivation of Computational Procedure

5.2.1 Computation of Response for SDOF Oscillator

Nonlinear response of a single-degree-of-freedom oscillator may be determined using the Newmark beta method (8). The procedure is outlined below for an oscillator subjected to a translational motion at its base.

Motion of a single-degree-of-freedom oscillator (Fig. 5.1) can be expressed in terms of the displacement, v , of the system and, v_g , of the base motion. If the resistance is linear with the deflection, then the equation of motion is:

$$m\ddot{v} + c\dot{v} + kv = 0 \quad (5.1)$$

If the absolute displacement, v_t , is represented as the sum of v and v_g , then the relation reduces to:

$$m\ddot{v} + c\dot{v} + kv = -m\ddot{v}_g \quad (5.2)$$

If the resistance varies nonlinearly with the deflection, then the stiffness, k , may be replaced with the more general expression $k(v)$.

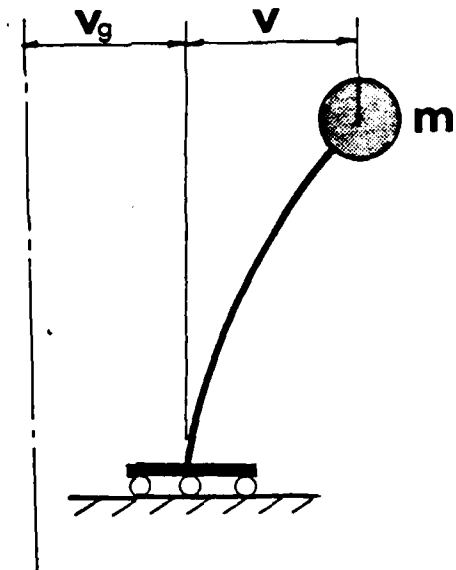


Fig. 5.1 Coordinates for Single-Degree-of-Freedom System

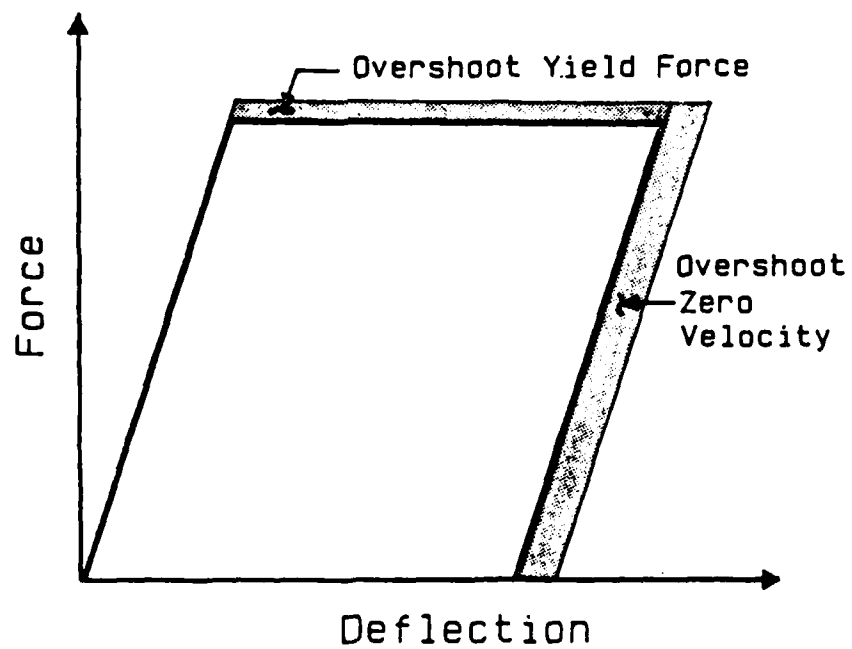


Fig. 5.2 Error Accumulation due to Overshoot

The nonlinear differential equation may be solved numerically for the unknown displacement, velocity or acceleration by considering the following kinematical relations which are based on a linearly varying acceleration across a time step:

$$\dot{v}_{n+1} = \dot{v}_n + (\ddot{v}_n + \ddot{v}_{n+1})h/2 \quad (5.3)$$

$$v_{n+1} = v_n + \dot{v}_n h + \ddot{v}_n h^2/3 + \ddot{v}_{n+1} h^2/6 \quad (5.4)$$

If an assumption is made of the acceleration at the end of a time step, \ddot{v}_{n+1} , then the velocity and displacement may be determined using these relations. Knowing the percentage of critical damping and the resistance function, the acceleration relative to the base, \ddot{v}_{n+1} , as a result of the input motion, \ddot{v}_g , may be determined by solving Eq. 5.2. The procedure may be iterated using the derived acceleration to determine velocity and displacement until convergence is reached.

Convergence of the iterative process will occur if the time step is less than 10% of the natural period of the elastic oscillator. For nonlinear systems, the time step should be no greater than this value and must be reduced to capture changes in the resistance function, such as at cracking, yield or upon unloading. If this is not done, errors in the amount of energy dissipated will tend to accumulate (Fig. 5.2). A simple algorithm is used which revises the time step in direct proportion to the amount of overshoot and the change in resisting force between two time steps.

$$h_{n+1} = h_n (R_n - R_a) / (R_n - R_{n-1}) \quad (\text{Eq. 5.5})$$

where R_a is the characteristic force separating two linear ranges of resistance. The time step is reduced for each iteration that exceeds a bound until the resisting force matches the idealized model, or when the velocity changes sign and unloading occurs.

An alternate procedure is to express the resistance function in terms of a smooth curve rather than a combination of piece-wise linear segments. Unless a drastic change in slope occurs such as at unloading, there is no need to change the time step. If the numerical algorithm is based on convergence of an assumed acceleration, then a resisting force may be expressed directly as a function of deflection. Although this procedure involves one or two iterations per time step, it eliminates the need to rely on estimating resistance with a tangent stiffness which may result in overshoot problems. The attractiveness of the procedure lies in the fact that the first derivative of the force-deflection curve is not required.

The calculation procedure is simple in that it marches in time with only having to remember the last instant of response. For nonlinear resistances

that are path dependent, it is necessary to remember a few other critical parameters to define the loading history. In any case, the method is well suited to a simple computational device such as a desktop computer with a single disk drive.

5.2.2 Generalized Formulation of Hysteretic Resistance

Former path-dependent models for hysteretic resistance functions have been developed to represent one, or a few, aspects of nonlinear behavior for a particular form of component. Some of these formulations have included simple bilinear, or elasto-plastic models such as the stiffness degrading model (Fig. 5.3b) proposed by Clough and Johnston (15), the modified Takeda (16) softening model (Fig. 5.3c) which includes a reduction in stiffness for unloading, and a slip-softening model (Fig. 5.3d) which has been used by Abrams and Tangkijngamvong (17).

Each of these models has been based on a set of linear segments joined at points with an abrupt angle change. Whereas through proper choice of slopes and connecting points, these models may be suitable for dynamic response calculations, the numerical integration process is cumbersome because care must be taken to properly define the time step so that over or under shoots may not be significant at concentrated points of curvature. A new formulation has been developed as part of this project which uses smooth curves to represent the resistance function, and is sufficiently general to encompass all, or any combination, of the previous hysteresis formulations.

The formulation used for the analysis establishes a new path once a change in the sign of the velocity is detected. The path is composed of both cubic and linear segments (Fig. 5.4). Control points which define the shape of the path are selected based on rules established from past or new formulations. Four segments are used to describe (a) linear unloading, (b) softening upon reversal of force, (c) gradual softening upon closure of cracks followed by softening at large forces, and (d) strength after yield of reinforcement. The cubic-spline model is most useful for representing portion (c) of the path. The rounded nature of the curve tends to become more pronounced as the separation between points B and C becomes larger. This mathematical property is closely related to what happens physically in a reinforced concrete member or connection as a result of crack closure at low amount of force, and the Bauschinger effect in the reinforcement at larger amounts of force.

The example path shown in Fig. 5.4 depicts that of a structure influenced by a slip mechanism such as for an interior beam-column joint. When force is reversed in direction cracks tend to close and reinforcing bars tend to slip back to original positions, thus resulting in a substantial decrease in stiffness. When the cracks are fully closed, and the reinforcing

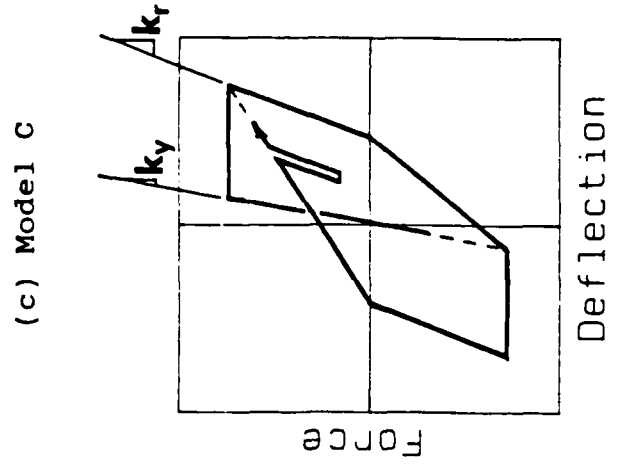
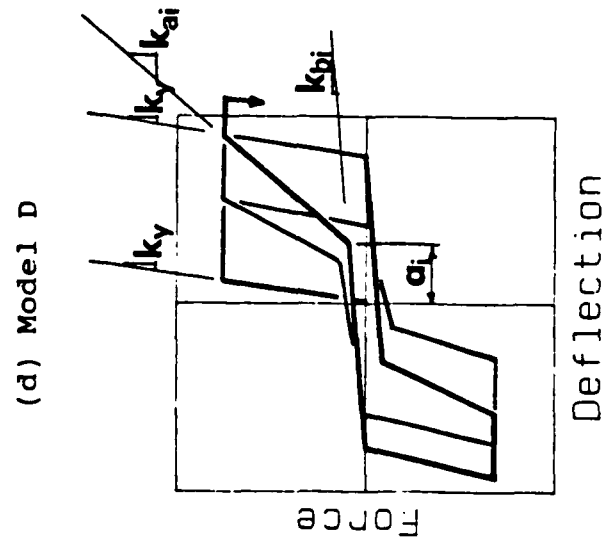
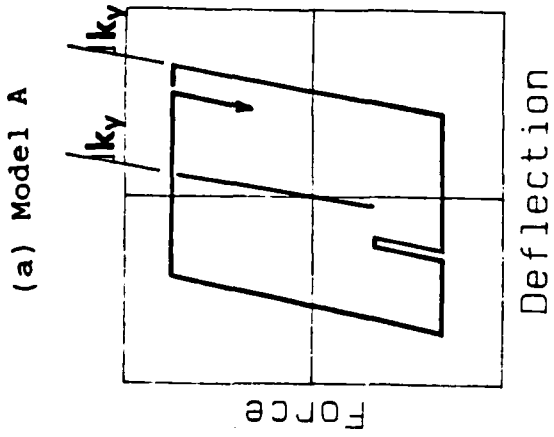
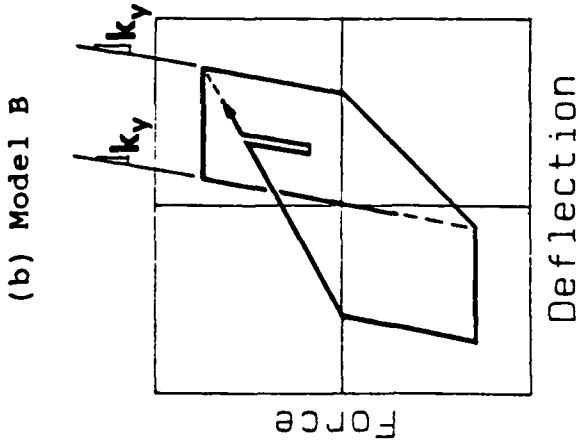
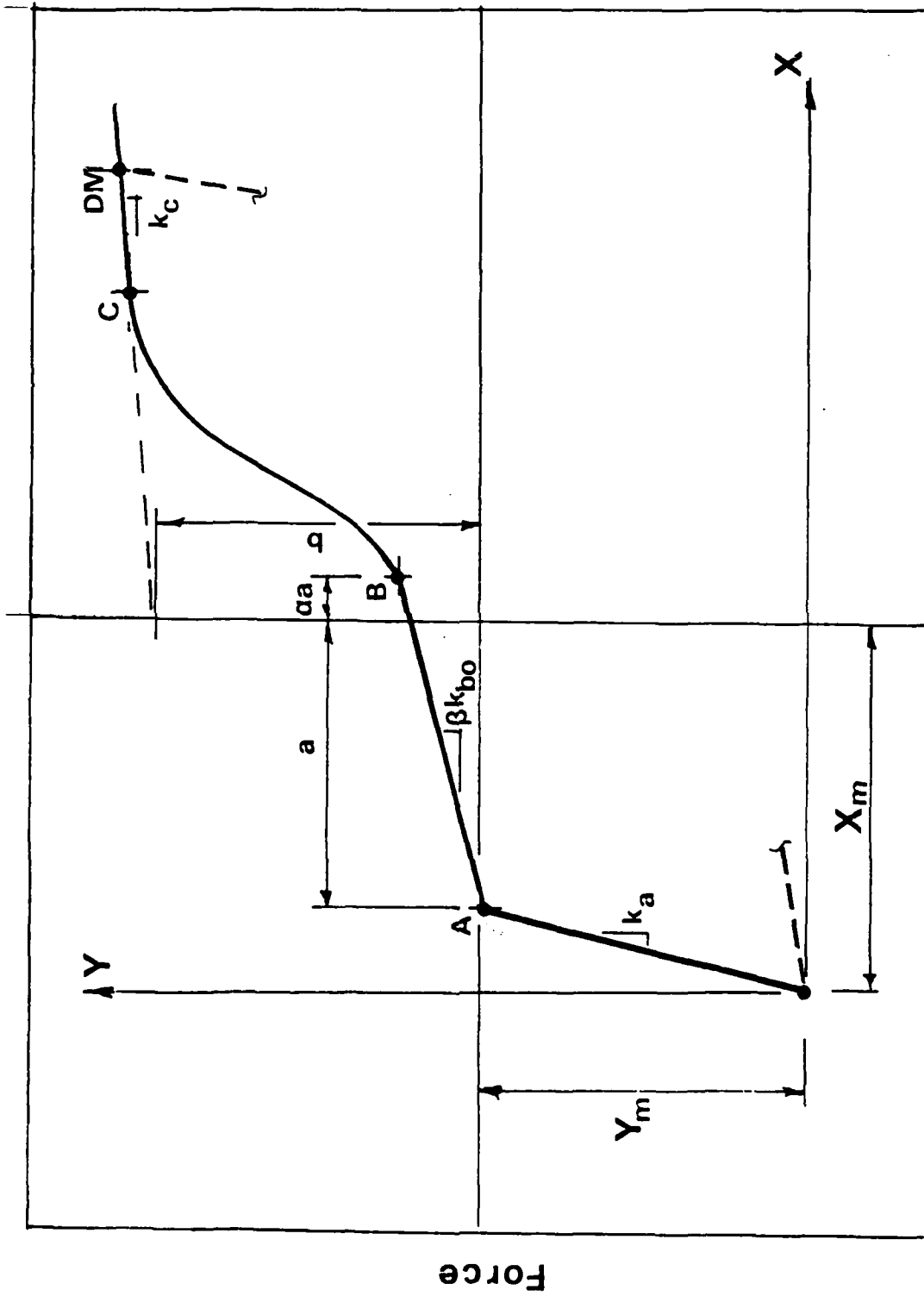


Fig. 5.3 Hysteresis Models used in Analysis



Deflection

Fig. 5.4 Cubic-Spline Hysteresis Model

bars develop anchorages for the new direction of force, the structure is observed to stiffen appreciably. Initially, the stiffness between points A and B is that for a section comprised of solely reinforcement, k_{bo} . As the member is cycled, bond is weakened which reduces this stiffness. The deterioration in stiffness which is represented with the term, β , is related to the amplitude of cycling and the number of cycles. As a simple approximation, the deterioration is expressed in terms of the previous deflection maxima for the same sense of forcing, DM, (Fig. 5.4). At a prescribed value of deflection, DBL, all bond is assumed to be lost, and the stiffness upon reversal of the force is taken as zero. The deflection at stiffening which is represented with the factor " α ", can also be related to this deflection ratio. A member will stiffen at a zero rotation if cracks do not open before the old ones close. If there has been a substantial amount of bond deterioration in an interior beam-column joint as discussed in Sec. 4.2, the tensile bars may slip from the joint as the compressive bars are pushed into the joint. This form of behavior is modeled with the simple relation shown in Fig. 5.5b.

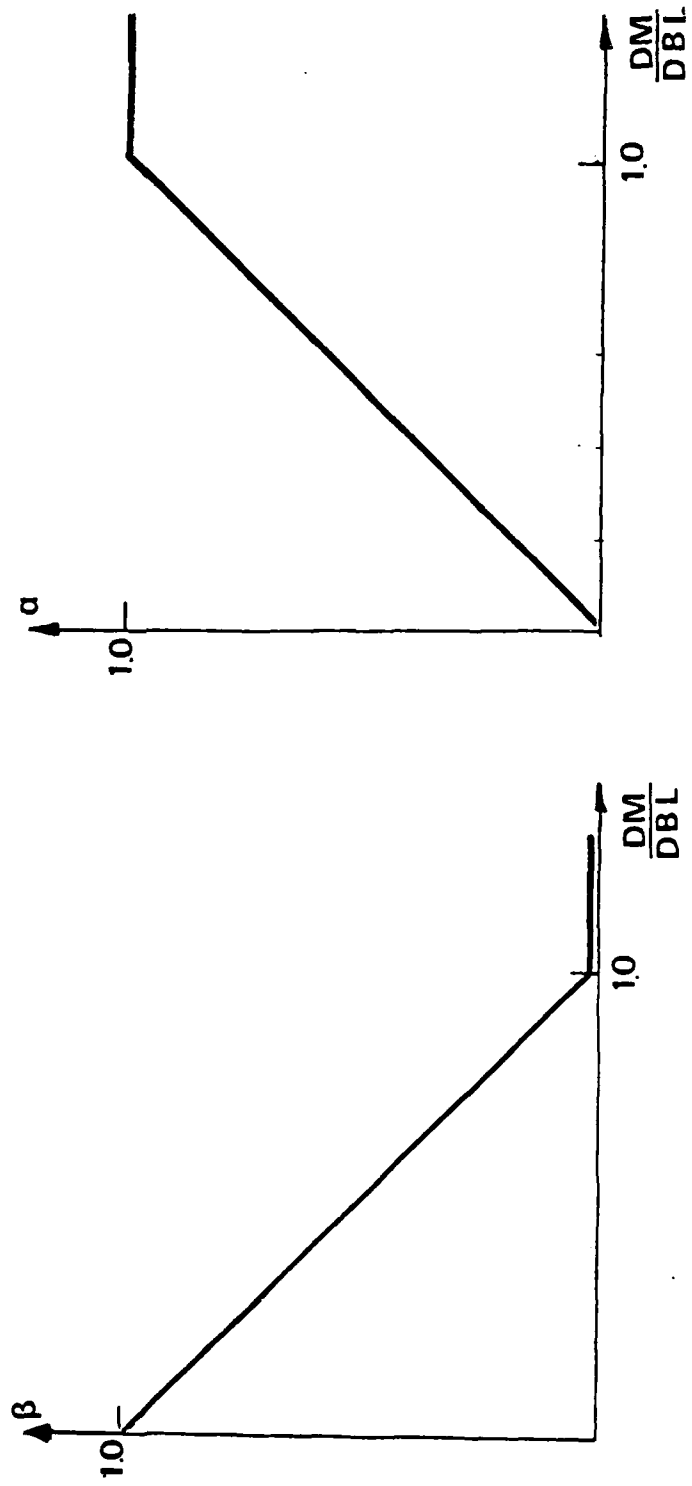
If the structure does not contain significant slip mechanisms such as for a wall responding in flexure with well anchored vertical steel, the stiffness from points A to B should be represented without the idealization just described. For this case, the member would respond with the stiffness of the previous unloading slope, k_a , or a value slightly less to model some slight crack closure. If a stiffness, k_b , is prescribed by the user that is greater than the average stiffness between points A and C, then the linear segment AB is eliminated from the path. The resulting path is similar to that modeled with a Ramberg-Osgood representation.

Because response to an earthquake motion may include several changes in velocity for a single nonlinear cycle, the algorithm must also account for reversals that are localized in one region of the curve. Linear behavior has been assumed if the member is unloaded and then reloaded before a change in the sign of the force has been reached (Fig. 5.6a). If the member is reloaded after a change in the sign of the force occurs, but not a change in sign of the deflection, then the member reloads with a single change in stiffness without slip (Fig. 5.6b).

Modeling of hysteretic behavior for concrete elements is still at the state-of-the-art in structural engineering. To help the user understand a particular hysteresis model before implementation in a dynamic analysis, a subroutine has been included with the program which permits the user to define deflection histories interactively with the right and left arrows. The force-deflection history is shown on the screen as the user controls the sequence of the deflections.

5.2.3 Earthquake Ground Motions

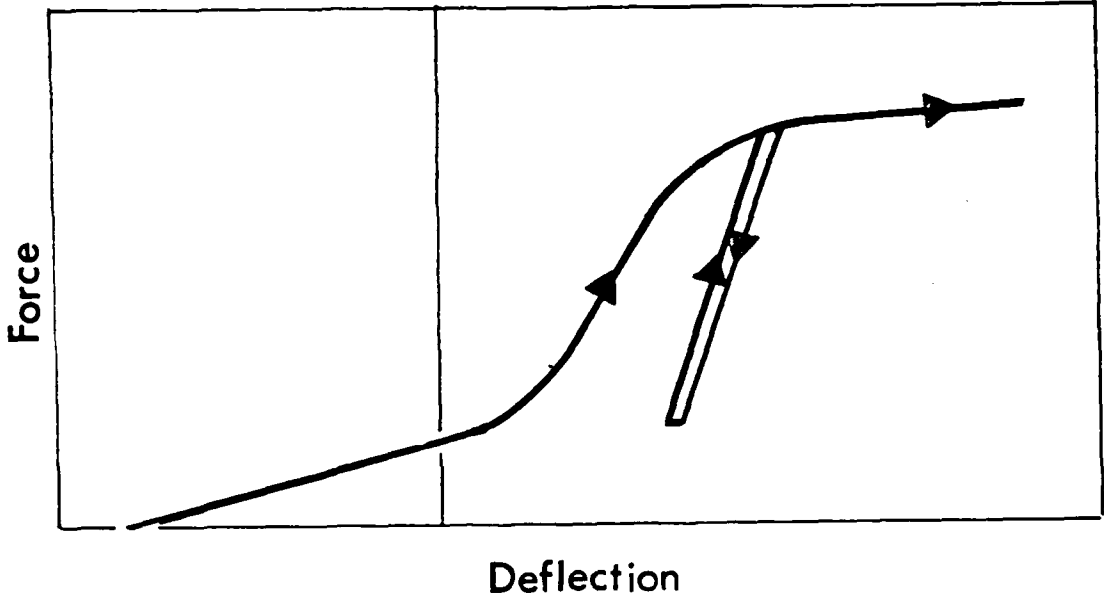
A library of recorded earthquake motions is compiled on diskette from the USGS data base. The user can select particular earthquake motions from a menu shown on the screen. He or she has the options of selecting one portion



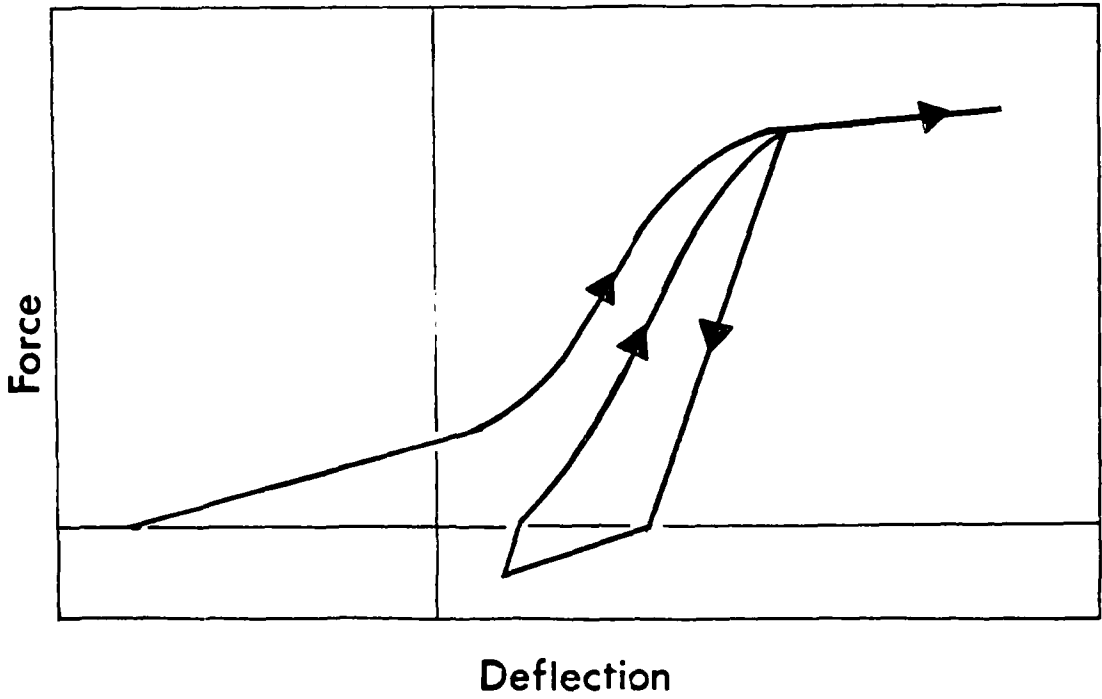
(a) Stiffness Deterioration

(b) Deflection at Crack Closure

Fig. 5.5 Idealizations for Bond Deterioration



(a) Before Changing Sense of Force



(b) Before Changing Sense of Deflection

Fig. 5.6 Rules for Reloading

of the motion, compressing the duration, and altering the maximum acceleration. The present file of motions contains the following earthquake records.

- (a) Imperial Valley, CA; El Centro; NS
- (b) San Fernando, CA; Pacoima Dam; S16E
- (c) San Fernando, CA; Castaic; N21E
- (d) San Fernando, CA; 3710 Wilshire; 10 Floor
- (e) Parkfield, CA; Temblor; S25W
- (f) Kern Co., CA; Santa Barbara Courthouse; S48E
- (g) Parkfield, CA; Cholame, Shandon; N85E
- (h) Miyagi, Japan
- (i) Tokachi-Oki, Japan

It is also possible for the user to link with existing data bases via a modem. Present software such as "EARTHQUAKE LOADING" and "OPTIREC" can be used for this purpose if development is done to convert these programs for use on a microcomputer. Other existing software such as "CH42" for selecting an earthquake motion given the site location can be used as well if this development is done. If recorded motions are not available at a particular site, ground motions can be synthesized using "SIMQKE" which generates statistically independent accelerograms from an input response spectra.

5.2.4 Modal Decoupling Procedure

Nonlinear response analysis for systems with many degrees of freedom becomes difficult because of the need to update and invert the stiffness matrix for every iteration of a particular time step. Furthermore, a complete history of deformation for every member in the structure must be remembered. Because execution speed and possibly storage requirements may make this computation unfeasible for present personal computers, an approximate procedure to reduce the number of degrees of freedom is proposed.

For uniform building structures whose response is dominated by the fundamental mode, it is feasible to express response in terms of a single generalized coordinate even though substantial nonlinear deformations have occurred. Tests of one-twelfth scale models (3) showed that distributions of displacement along the height were quite similar for all ranges of response. Modal participation factors calculated from measured deflected shapes varied within 5% for large and small-amplitudes of motion. Because displacement response was governed by the fundamental mode, lateral displacements at any particular level could be represented by a single dynamic degree of freedom and a single distribution function.

Although higher modes can be represented in the same way, the simplified approach is not applicable for systems with a large participation of higher

modes because superposition is not valid for nonlinear systems. The approach to be used, therefore, applies only to buildings that would vibrate in the fundamental mode: usually low rise structures not exceeding ten stories in height.

To use the nonlinear analysis procedure described previously for a single-degree-of-freedom system, physical properties of the structure must be translated to properties associated with a given generalized coordinate. For purposes of simplicity, this shall be considered as the lateral displacement at the top level, Z_n . Knowing the amounts and distribution of mass along the height of structure, and a specified displacement shape, an equivalent mass can be determined which if placed at the tenth level would result in the same internal forces. This operation is based on conventional modal decoupling procedures which are summarized below.

The equation of motion for a multi-degree-of-freedom system may be expressed as:

$$[M]\{\ddot{v}^t\} + [C]\{\dot{v}\} + [R(v)] = \{0\} \quad (\text{Eq. 5.6})$$

where $[M]$ is the mass matrix which is diagonal for a system of lumped masses, $[C]$ is the damping matrix, and $[R(v)]$ is the set of resisting forces that vary nonlinearly with the relative displacements, $\{v\}$. The resisting forces may be expressed in terms of dynamic and static degrees of freedom and a stiffness matrix. For a rigorous analysis, this matrix must be updated and inverted for each iteration of a particular time step which results in a lengthy computation. Because the proposed technique simplifies the system to one degree of freedom, assembly of the stiffness matrix is not required. For this reason, the resisting forces are expressed simply in terms of a column vector.

The total acceleration at each level, $\{\ddot{v}^t\}$, may be decomposed to motions of the ground, $\{\ddot{v}_g\}$, and relative motions of the structure to the ground, $\{\dot{v}\}$:

$$[M]\{\ddot{v}\} + [C]\{\dot{v}\} + \{R(v)\} = -[M]\{r\}\ddot{v}_g(t) \quad (\text{Eq. 5.7})$$

Components of the $\{r\}$ vector are displacements of a rigid structure due to unit motions of the ground. This vector is equal to $\{1\}$ for a system of lumped masses along a vertical line which is subjected to translation at the base.

The motions of each floor level may be expressed in terms of the summation of products of distribution functions and generalized coordinates:

$$\{v(x,t)\} = [\Phi(x)]\{Z(t)\} \quad (\text{Eq. 5.8})$$

where $[\Phi(x)]$ is a composite of individual modal shapes, $\{\phi_n(x)\}$, and $\{Z(t)\}$ is a series of modal amplitudes, $Z_n(t)$. If modal shapes have been normalized with respect to the top level, $Z_n(t)$ is both the modal and top-level displacement. Substitution of this relation in Eq. 5.7 results in the following relation:

$$[M][\Phi]\{\ddot{Z}(t)\} + [C][\Phi]\{\dot{Z}(t)\} + \{R(v)\} = -[M]\{r\}\ddot{v}_g(t) \quad (\text{Eq. 5.9})$$

This set of equations can be decoupled to a single scalar equation by premultiplying each term by $\{\phi_n\}^t$, and invoking the following orthogonality relation with respect to the mass matrix.

$$\{\phi_m\}^t [M] \{\phi_n\} = 0 \quad (\text{Eq. 5.10})$$

Furthermore, it is required that the damping matrix, $[C]$ is proportional to the mass matrix so that a similar orthogonality condition may result. Although this assumption is not precisely correct, its use is justified for systems with large nonlinear deformations. These systems dissipate most of the energy through hysteretic effects related to deflections. Viscous damping mechanisms occur at large velocities which occur at small displacements within the linear range of response.

The uncoupled scalar equation for mode n is:

$$M_n \ddot{z}_n + C_n \dot{z}_n + \{\phi_n\}^t \{R(v)\} = -\{\phi_n\}^t [M] \{1\} \ddot{v}_g(t) \quad (\text{Eq. 5.11})$$

where M_n , the generalized mass is equal to $\{\phi_n\}^t [M] \{\phi_n\}$. For a lumped mass system the mass matrix is diagonal, and M_n may be expressed using summation notation as:

$$M_n = \{\phi_n\}^t [M] \{\phi_n\} \quad (\text{Eq. 5.12})$$

Because only the fundamental mode is of interest, the generalized mass, M_1 may be determined from a distribution of lateral deflection for the first mode, $\{\phi_1\}$. For structural systems with uniform mass and stiffness distributions, a triangular or parabolic shape may be sufficiently precise for determination of M_1 . For systems with irregular distributions, the first mode shape should be obtained from an eigenvalue solution. The shape may also be derived from a linear static analysis which is based on an assumed lateral force distribution. Subsequent analyses can be done using the derived deflected shape as the lateral force distribution until the exact modal shape is obtained. This method is known as the Rayleigh Method which is described in (7).

The modal damping, C_n , may be expressed in terms of the percentage of critical damping, ξ_n as follows:

$$C_n = 2M_n \omega_n \xi_n \quad (\text{Eq. 5.13})$$

This relation is based on elastic behavior, however, viscous effects are significant at small displacements which are usually elastic.

The modal resisting force, $\{\phi_n\}^t \{R(v)\}$, can be deduced from the base shear at a particular amplitude of top-level deflection. When an undamped multi-degree-of-freedom system is in free vibration, the resisting forces within the structure are in equilibrium with the inertial forces according to the following relation.

$$\{R(v)\} = [M]\{\ddot{v}\} \quad (\text{Eq. 5.14})$$

Or, for a particular mode, n ,

$$\{R_n(v)\} = [M]\{\phi_n\}\ddot{Z}_n \quad (\text{Eq. 5.15})$$

The base shear for a particular mode, V_{bn} , is the summation of these forces. In matrix notation:

$$V_{bn}(z) = \{1\}^t \{R_n(v)\} = \{1\}^t [M]\{\phi_n\}\ddot{Z}_n \quad (\text{Eq. 5.16})$$

Solving this equation for \ddot{Z}_n , and substituting in Eq. 5.15:

$$\{R_n(v)\} = ([M]\{\phi_n\}/\{1\}^t [M]\{\phi_n\})V_{bn}(z) \quad (\text{Eq. 5.17})$$

Premultiplying by $\{\phi_n\}^t$ to obtain the modal quantity in Eq. 5.11, and noting the definition of modal mass, M_n , from Eq. 5.12:

$$\{\phi_n\}^t \{R_n(v)\} = (M_n/\{1\}^t [M]\{\phi_n\})V_{bn}(z) \quad (\text{Eq. 5.18})$$

Substitution of all expressions in Eq. 5.11 and dividing by M_n :

$$\ddot{Z}_n + 2\omega_n \xi_n \dot{Z}_n + V_{bn}(z)/\{1\}^t [M]\{\phi_n\} = -(\{\phi_n\}^t [M]\{1\}/M_n)\ddot{v}_g$$

$$(\text{Eq. 5.19})$$

Eq. 5.19 may be nondimensionalized by introducing $\Psi_n(z)$, which is the ratio of the base shear to the weight of the structure. If the weight of the structure is expressed in matrix form as:

$$W = \{1\}^t [M] \{1\} g$$

then the third term in Eq. 5.19 may be expressed as:

$$\beta_n \Psi_n(z) g$$

where β_n is equal to $\{1\}^t [M] \{1\} / \{1\}^t [M] \{\phi_n\}$. If α_n is used to represent the coefficient of \ddot{v}_g in Eq. 5.19, which is more commonly known as the modal participation factor, then Eq. 5.19 simplifies to:

$$\ddot{z}_n + 2\omega_n \xi_n \dot{z}_n + \beta_n \Psi_n(z) g = -\alpha_n \ddot{v}_g \quad (\text{Eq. 5.20})$$

To solve the above equation, the following parameters need to be defined:

- (a) the mass distribution
- (b) an assumed deflected shape
- (c) percentage of critical viscous damping
- (d) an estimate of the modal period
- (e) ratio of base shear to total weight when structure is deflected to a specific top-level deflection
- (f) type of hysteresis formulation.

Note that knowledge of the total amount of mass is not required because the base shear is normalized with respect to this quantity in the Ψ_n term.

For many buildings, the distribution of mass is uniform and α_n and β_n reduce to functions of solely the deflected shape. These two factors have been determined for this case considering a triangular shape, and two parabolic shapes which represent bounds on possible shapes. Results are summarized for different building heights in Table 5.1. The β_n factor is more sensitive to the shape assumption than is the factor, α_n . Both factors converge to a constant value as the number of stories increases, however, the ratio of the factors, or the relative amount of applied force without consideration of damping or inertia, converges much more rapidly than the individual factors. This implies that if the structure is taller than a few stories, the number of stories has very little relevance to the analysis. Furthermore, the sensitivity of the calculation to the assumption of deflected shape is bounded in terms of the spread of these ratios for flexure beams and shear beams: a range equal to 0.6 to 0.9.

Table 5.1

PARTICIPATION FACTORS BASED ON DEFLECTED SHAPE

No. of Stories	ALPHA			BETA Shape Assumptions			ALPHA/BETA		
	F	T	S	F	T	S	F	T	S
1	1.00	1.00	1.00	1.00	1.00	1.00	1.00	1.00	1.00
2	1.18	1.20	1.12	1.60	1.33	1.14	0.74	0.90	0.98
3	1.29	1.29	1.16	1.93	1.50	1.23	0.67	0.86	0.95
4	1.36	1.33	1.19	2.13	1.60	1.28	0.64	0.83	0.93
5	1.40	1.36	1.20	2.27	1.67	1.32	0.62	0.82	0.91
6	1.44	1.38	1.21	2.37	1.71	1.34	0.61	0.81	0.90
7	1.47	1.40	1.21	2.45	1.75	1.36	0.60	0.80	0.89
8	1.49	1.41	1.22	2.51	1.78	1.38	0.59	0.79	0.89
9	1.51	1.42	1.22	2.56	1.80	1.39	0.59	0.79	0.88
10	1.52	1.43	1.23	2.60	1.82	1.40	0.59	0.79	0.88
15	1.56	1.45	1.23	2.72	1.88	1.43	0.57	0.77	0.86
20	1.59	1.46	1.24	2.79	1.90	1.45	0.57	0.77	0.86
25	1.60	1.47	1.24	2.83	1.92	1.46	0.57	0.76	0.85
30	1.61	1.48	1.24	2.86	1.94	1.46	0.57	0.76	0.85

$$\text{ALPHA} = \frac{\sum \Phi_i}{\sum \Phi_i^2}$$

$$\text{BETA} = \frac{N}{\sum \Phi_i}$$

'F' = Parabolic Flexure Beam

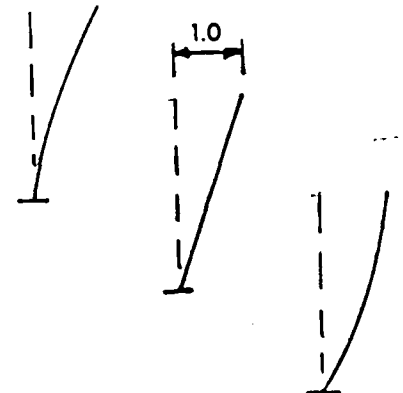
$$\Phi_i = \frac{i^2}{N^2}$$

'T' = Triangular Shape

$$\Phi_i = \frac{i}{N}$$

'S' = Parabolic Shear Beam

$$\Phi_i = 1 - \frac{(N-i)^2}{N^2}$$



Items (c) and (d) are used to determine the viscous damping force. Uncertainty is related to the product of these two values, and not to their separate values. For this calculation, the accuracy of the frequency should only be as good as the estimate of damping percentage. During large inelastic displacements, the velocity is usually small, and the effect of this term on overall response is not significant.

The resisting force is represented with item (e). The relation between base shear and top-level deflection (Fig. 5.7) needs to be obtained. Behavior under monotonically increasing forces may be assumed to represent the envelope for cyclic loadings. The remainder of the force-deflection relation is based on this "spinal curve" using the hysteresis formulation specified in item (f). The selection of hysteresis type is based on judgement of the analyst. Several reports have been published that describe measured behavior of concrete components and structures under force reversals. Most of these test results fit a particular hysteresis formulation (Figs. 5.3) included in the program, however, the user is free to develop his or her own rules. Because changing the hysteresis type requires a small investment in effort, several analyses can be run to examine the sensitivities of response to this parameter.

5.3 Application of Technique

5.3.1 Introductory Remarks

The essential part of the computational technique is a routine that determines nonlinear response of a single-degree-of-freedom oscillator to any time-dependent loading. Application of the technique is arbitrary and depends on the needs of the user. Sophistications are dependent on the precision of the nonlinear force-deflection assumption.

A flow-chart of the overall technique is provided in Fig. 5.8. Nonlinearities of the structure are specified in terms of the relation of base shear to top-level displacement. This relation may be approximated for a rapid analysis, or defined in terms of the sequence of plastic hinge formation using a static lateral analysis of the structure. Each of these two approaches are described in the subsequent two sections. The computer program provides the user with several options for specification of input data, and preparation of output data. For typical building structures with uniform distributions of mass and stiffness, the user may choose default parameters which define the mode shape and mass matrix. For other structures, the user may define the mode shape and mass matrix.

In addition to waveforms of acceleration, velocity or displacement, the history of base-shear versus top-level deflection can be viewed on the screen. Sample output is shown in the Appendix. Each waveform may be scanned from the

keyboard to obtain numerical values of response at particular instants, or a complete listing of data may be printed. Results may also be plotted if report quality is desired. If selected, a set of equivalent lateral forces will be generated based on the inelastic response maxima. These forces may be used with a static analysis for member design.

5.3.2 Rapid Nonlinear Dynamic Analysis

It is often the case that a quick estimate of maximum response is necessary for a vulnerability assessment without knowing precisely the stiffnesses of the structure. There are also instances when a preliminary analysis is necessary to approximate a set of equivalent lateral design forces. A thorough description of the nonlinear force-deflection curve is not available, however it is still possible to perform a nonlinear dynamic analysis using a simple bilinear representation. Two parameters are required: the elastic stiffness and the base-shear capacity.

The stiffness can be obtained from an estimate of the fundamental mode frequency. This approximation can be estimated from the number of stories ($0.1N$), or in terms of the overall dimensions of the building such as prescribed with the following formula from the P355 manual.

$$T_a = 0.05h_n/\sqrt{L} \quad (\text{Eq. 5.21})$$

The period may be converted to the circular frequency,

$$\omega_1 = 2\pi/T_a \quad (\text{Eq. 5.22})$$

which when squared and multiplied by the generalized mass, M_1 , represents the modal stiffness, K_1 , for linear behavior. The product of K_1 times the generalized displacement, Z , is the resisting force, which may be used in lieu of the third term in Eq. 5.20.

The base shear strength can be approximated from a quick estimate of crosssectional areas and ultimate stresses as is suggested in the Rapid Seismic Analysis Procedure (18,19). Alternatively, base shear strength can be determined considering the internal virtual work resisted by the structure acting as a mechanism. In either case, the base shear strength can be expressed in terms of the nondimensionalized variable, $\psi_n(z)$, in Eq. 5.20, for all displacements greater than the proportional limit.

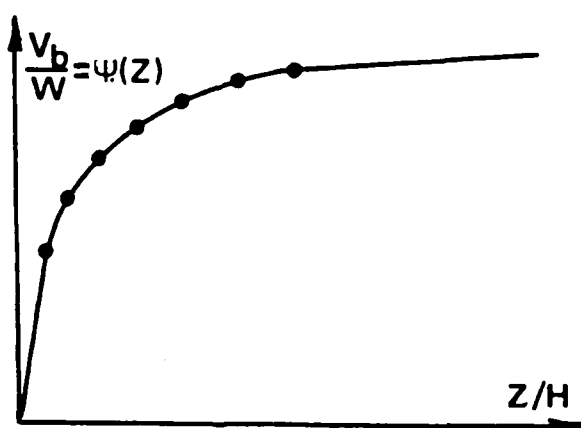
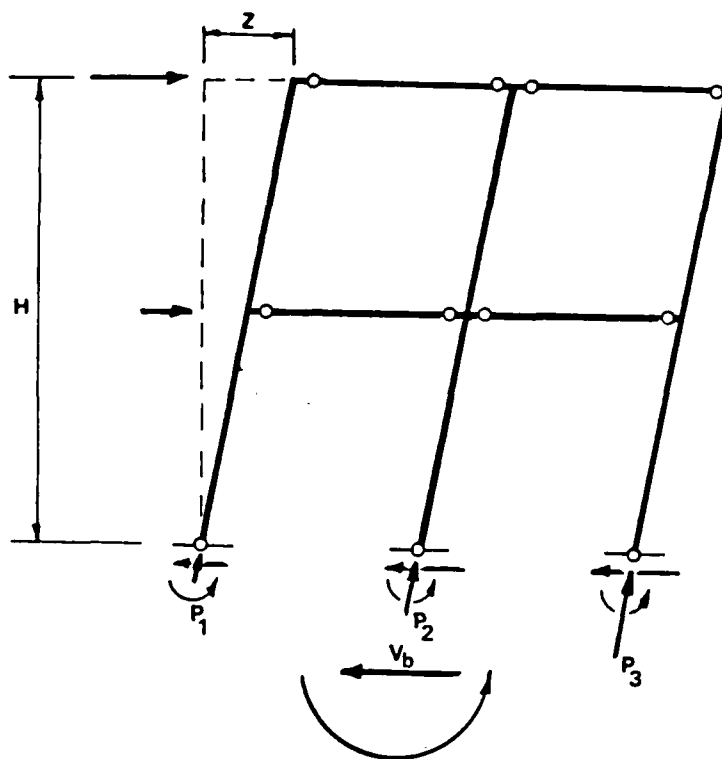


Fig. 5.7 Normalized Relation between Base Shear and Top-Level Deflection

Rapid Nonlinear
Dynamic Analysis

Explicit Consideration
of Stiffness Properties

A. Determine frequency and
base-shear capacity

A. Determine relation between
base shear and top deflection

- B. Specify mode shape:
triangular, flexure or shear beam, or
user defined
- C. Specify mass distribution:
uniform, or user defined
- D. Specify viscous damping:
user defined as percent of critical
- E. Select earthquake:
menu selection of typical motions, or
from CalTech data base via modem
- F. Select hysteresis formulation:
menu selection of bilinear, stiffness
degrading, softening, etc., or
user defined
- G. Execute program on PC:
response histories of displacement, velocity,
and/or acceleration will be displayed on
screen with history of base shear vs. top
deflection
- H. Select output options:
scan waveform on screen for numerical values,
print data file, print screen graphics, or
send to plotter
- I. Reduction of calculated waveforms:
required inelastic deformations, number
of inelastic cycles, damage indices, set
of lateral forces for static analyses of
member forces
- J. Select new input parameters, and re-execute

5.3.3 Explicit Consideration of Stiffness Properties

The previous rapid analysis technique is approximate because the stiffness characteristics of the structure are estimated without regard to materials, section sizes, or configuration. These parameters may be summarized with a single force-deflection curve for the entire structure. Using a piece-wise elastic analysis, the relation between base shear and top-level deflection may be obtained. The slope of the curve will reduce gradually as members in the structure yield. After all members yield, the curve will be horizontal at a value of base shear corresponding to the mechanism strength. This curve may be normalized with respect to the weight of the structure to provide input information in terms of $\Psi_n(z)$ in Eq. 5.19. It is assumed that behavior in all other ranges of the hysteresis curve will be related to this behavior upon loading. For asymmetrical structures, the spinal curve may be designated for each direction of loading.

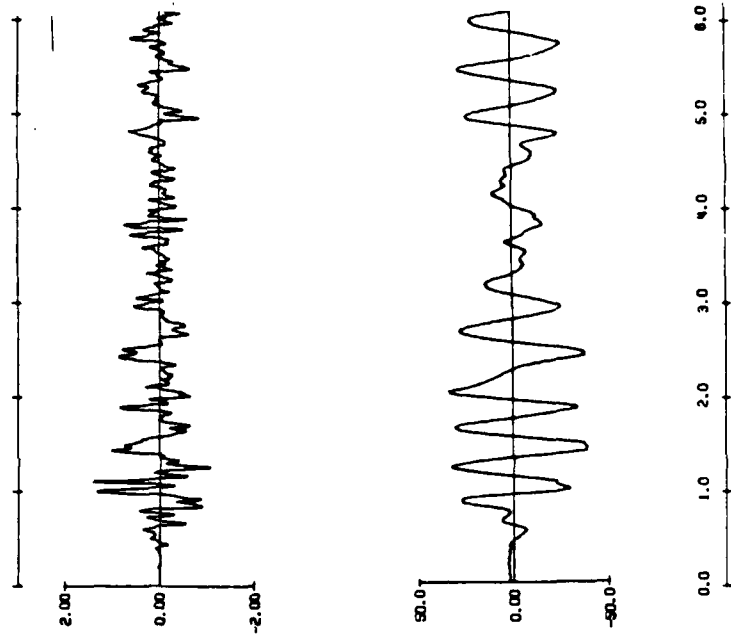
Because this analysis requires a linear static analysis of the structure, it is worthwhile to determine the fundamental mode shape and frequency rather than use the estimations of the previous method. For structures with nonuniform distributions of mass or stiffness, these calculations become essential.

6.0 Verification and Sample Results

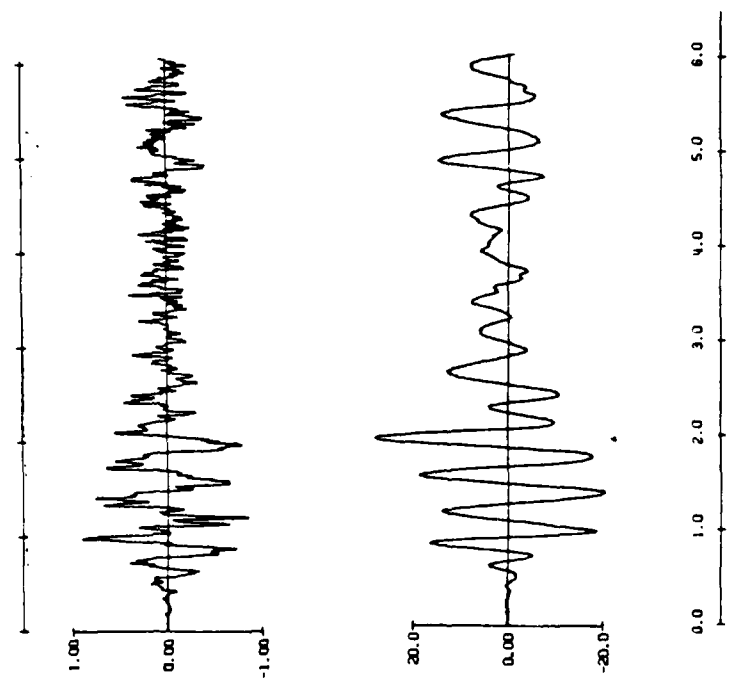
6.1 Verification of Procedure with Measurements

The procedure has been verified by comparing its results with that of a reduced-scale shaking-table model. The sample structure was a 10-story reinforced concrete frame-wall structure with an even distribution of mass at each level, and equal heights at each story. Further details of the test structure may be found in Ref. 3.

The measured deflected shape of the test specimen when subjected to simulated earthquake motions was mostly similar to the parabolic flexure beam idealization incorporated with the computer program. The maximum base shear was approximately 40% of the total weight. The lateral deflection at which the structure formed a mechanism can be estimated at 1.0% of the height. Stiffnesses at unloading were approximated with a value of 60 which was slightly greater than that for loading within the elastic range. Because the structure was fabricated with model materials, slippage of reinforcement should have been dominant on the cyclic behavior of the frames. For this reason, a low reversal stiffness of 5.0 which reduced to zero when a maxima deflection equal to six times the yield deflection was reached.



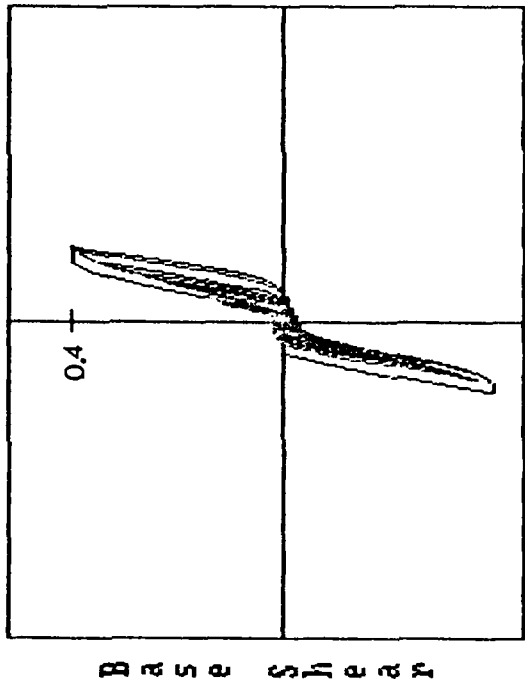
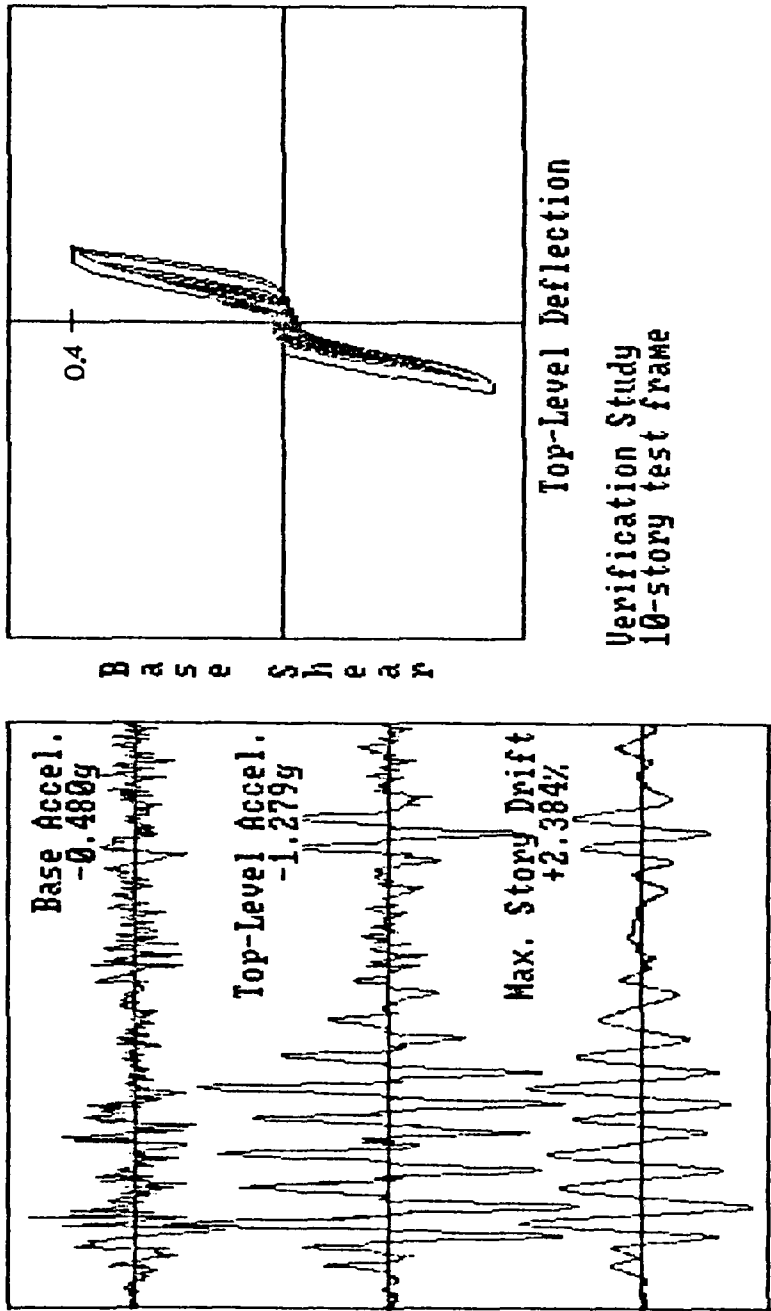
Run 1



Run 2

Fig. 6.1a Measured Response of Reduced-Scale Model

Imperial Valley Earthquake - May 18 1940 - El Centro - NS Time: 6.11 sec.



Top-Level Deflection

Verification Study
10-story test frame

Fig. 6.1b Response Computed with Simple Model - Run 1

Imperial Valley Earthquake - May 18 1940 - El Centro - NS Time: 6.12 sec.

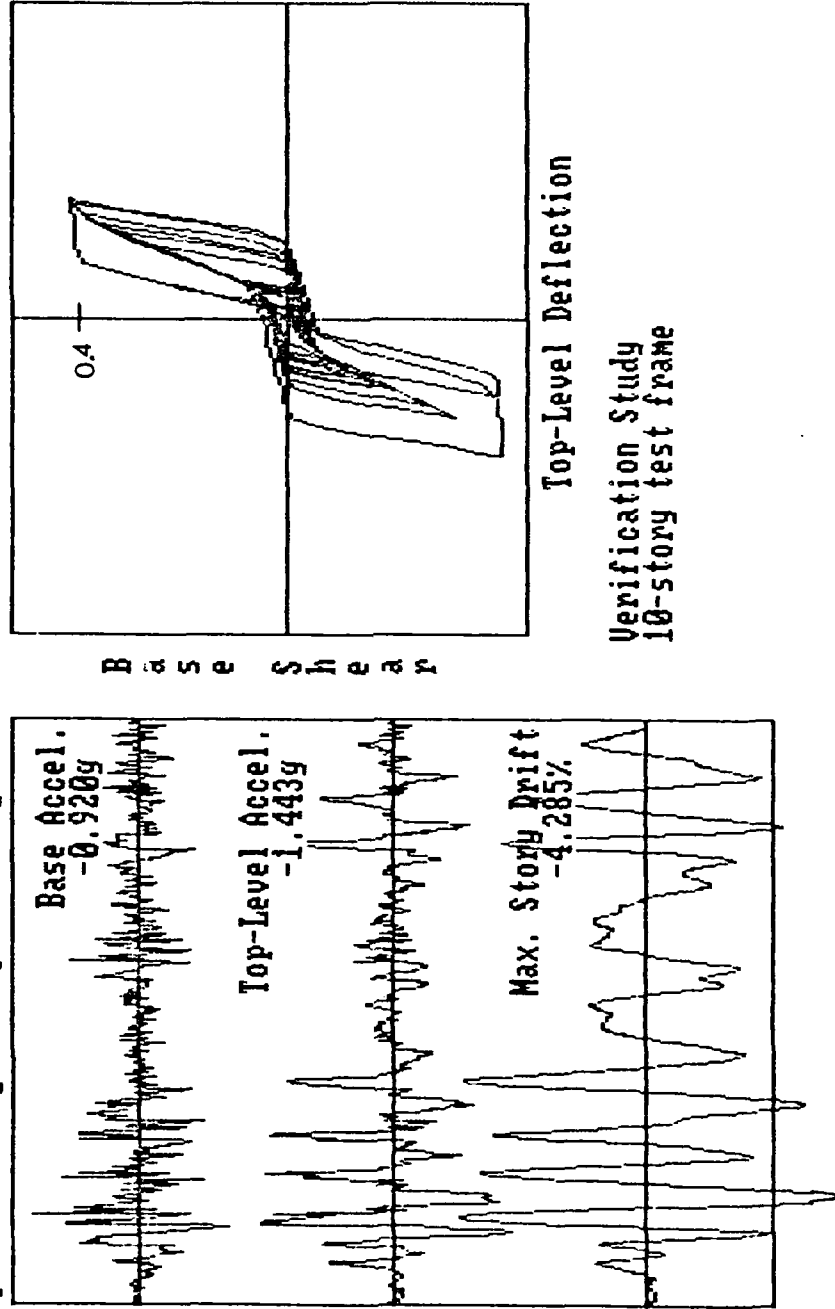


Fig. 6.1c Response Computed with Simple Model - Run 2

The motion input to the base of the test structures was a modeled version of the motion measured at El Centro, California during the 1940 Imperial Valley Earthquake. Duration of the record has been compressed by a factor of 2.5, and the maximum base acceleration was scaled to 0.48g and 0.92g. Because input information for the program is in a nondimensionalized form, only the time step was reduced by the 2.5 factor.

Measured response of the test structures is presented in Fig. 6.1a. Results of the analysis are shown in Fig. 6.1b and 6.1c for each of two intensities of base motion. Rather than maximum story drift, measurements are deflections at the tenth level. However, direct comparison can be made with the shape of response histories since calculated drifts are a fixed percentage of the top-level deflection.

Comparison of drift and acceleration maxima are summarized below.

	Run 1		Run 2	
	Measured	Calc.	Measured	Calc.
Max. Drift	2.30%	2.38%	3.35%	4.25%
Max. Accel.	0.91g	1.28g	1.47g	1.44g

The correspondence between measured and calculated values is within the intended range of accuracy for the simplified procedure. The large difference in drifts for Run 2 may be attributable to the fact that significant hinging occurred at the base. If a triangular deflected shape were assumed rather than the parabolic one, the calculated value of 4.25% would reduce to near the measured value.

The shapes of measured and calculated response histories are not in exact agreement, however, when viewed in terms of the stiffness assumptions made, the correlation is acceptable. The general pattern is replicated reasonably well in terms of the response maxima, and the number of cycles at a particular level of deflection.

In summary, the method is suitable for estimating the approximate pattern of nonlinear response for a building system with only rough estimates of its stiffness characteristics.

6.2 Sample Results of Procedure

Response has been calculated for a five-story, large-scale structure which is described in the sample input information supplied in the Appendix.

Response of the same structure to four different base motions is presented in Figs. 6.2 and 6.3. For these test cases, the strength-to-weight ratio used for the structure was 0.2. The reversal slope was a value of 5.0 to represent a "slip" type of hysteresis.

The input motions for response shown in Fig. 6.2 consisted of the first 8.0 seconds of the motion recorded at El Centro, California. The maximum acceleration of the motion was taken equal to the recorded 0.35g (Fig. 6.2a) as well as 0.60g (Fig. 6.2b). It is interesting to note that because of the increased amount of nonlinearity with the more intense motion, accelerations were about the same. Drifts did increase in like proportion to the maximum base accelerations. The sequence of the response and the number of cycles at large deflections, however, was much different for the each of the structures.

Response shown in Fig. 6.3 is a result of ground motions recorded at Tokachi-Oki and Miyagi, Japan. The frequency content of these motions differs substantially from that of the El Centro motions. Much more energy was released from these motions as can be inferred from the relatively large areas under the accelerograms. As a result, deflections and amounts of nonlinear behavior were quite large for the smaller base accelerations. As for the El Centro structures, amplification of base acceleration was small because of the hysteretic energy dissipation and progressive softening of each structure.

Response shown in Fig. 6.4 represents that for a structure without "slip" mechanisms, or a typical wall type building. The strength ratio has been changed from 0.2 to 0.4 to represent conceptually the case of strengthening a building system. Base motions for each case are those measured at El Centro, California. Care must be taken in comparing waveforms because deflections have been scaled in accordance with values at yield which differ by a factor of two.

The important feature of the comparison is that the strengthened structure deflects, and accelerates more than the unstrengthened one. The implication is that a nonlinear analysis, though simple and approximate, can eliminate the need to strengthen a building.

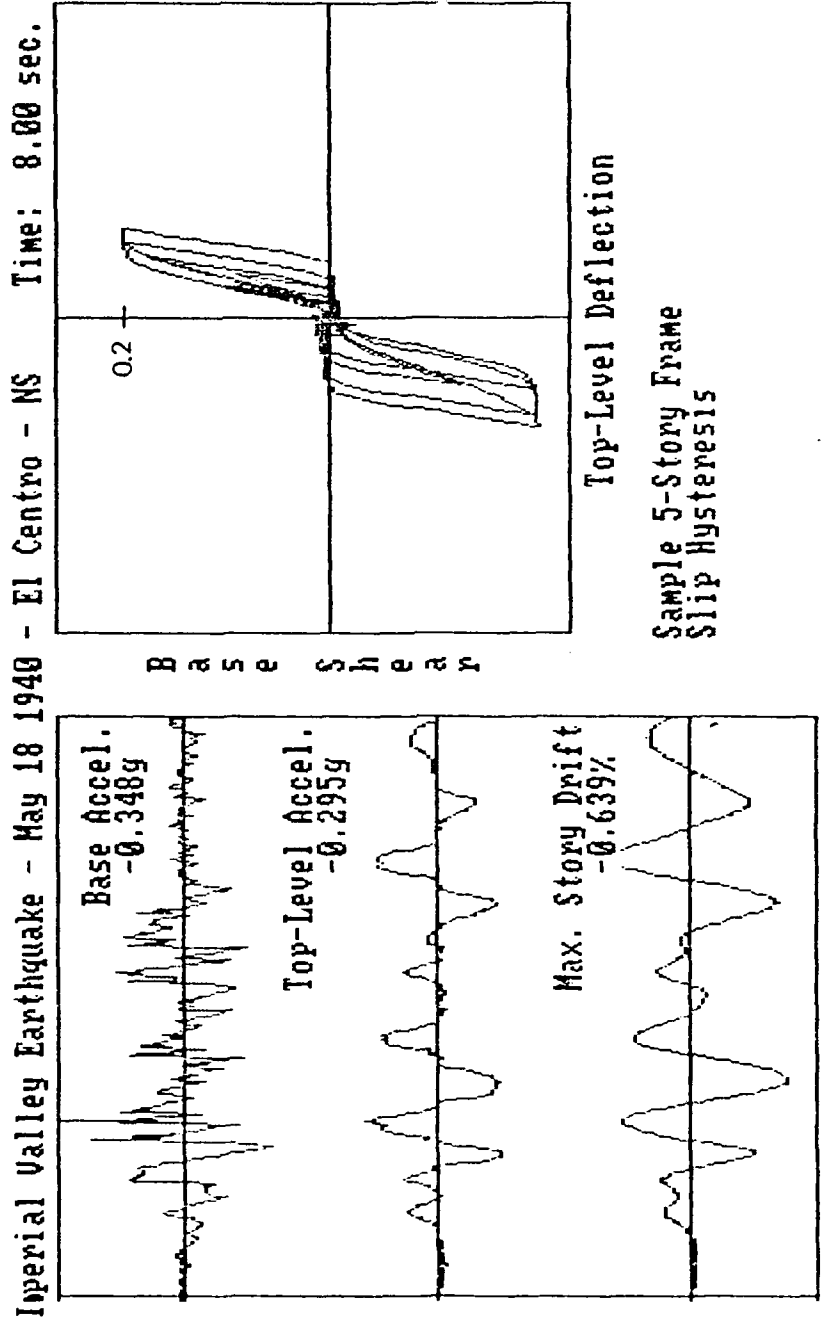
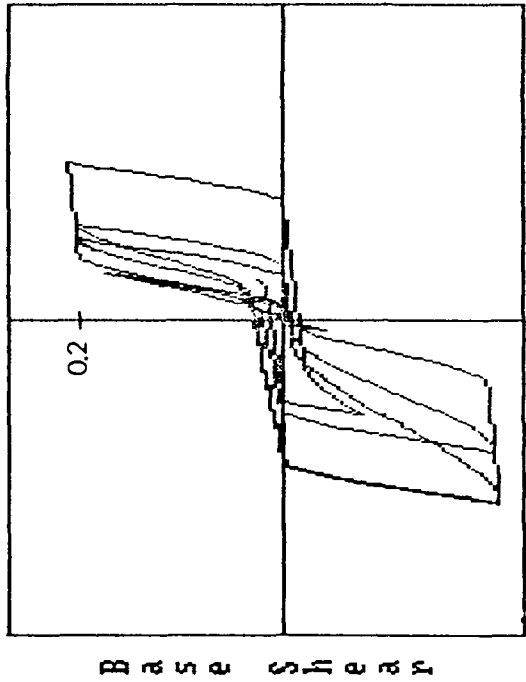
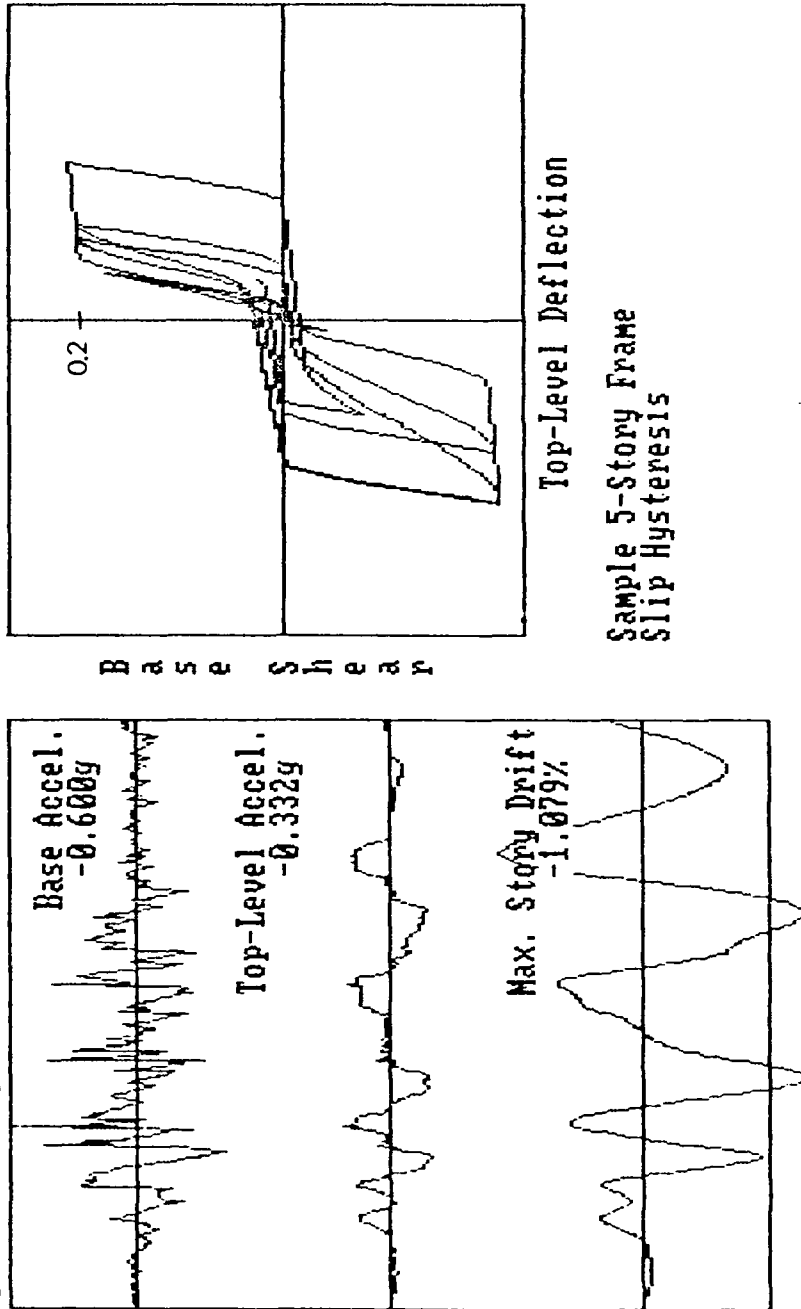


Fig. 6.2a Computed Response to El Centro, 0.348g

Imperial Valley Earthquake - May 18 1940 - El Centro - NS Time: 8.01 sec.



Top-Level Deflection

Sample 5-Story Frame
Slip Hysteresis

Fig. 6.2b Computed Response to El Centro, 0.600g

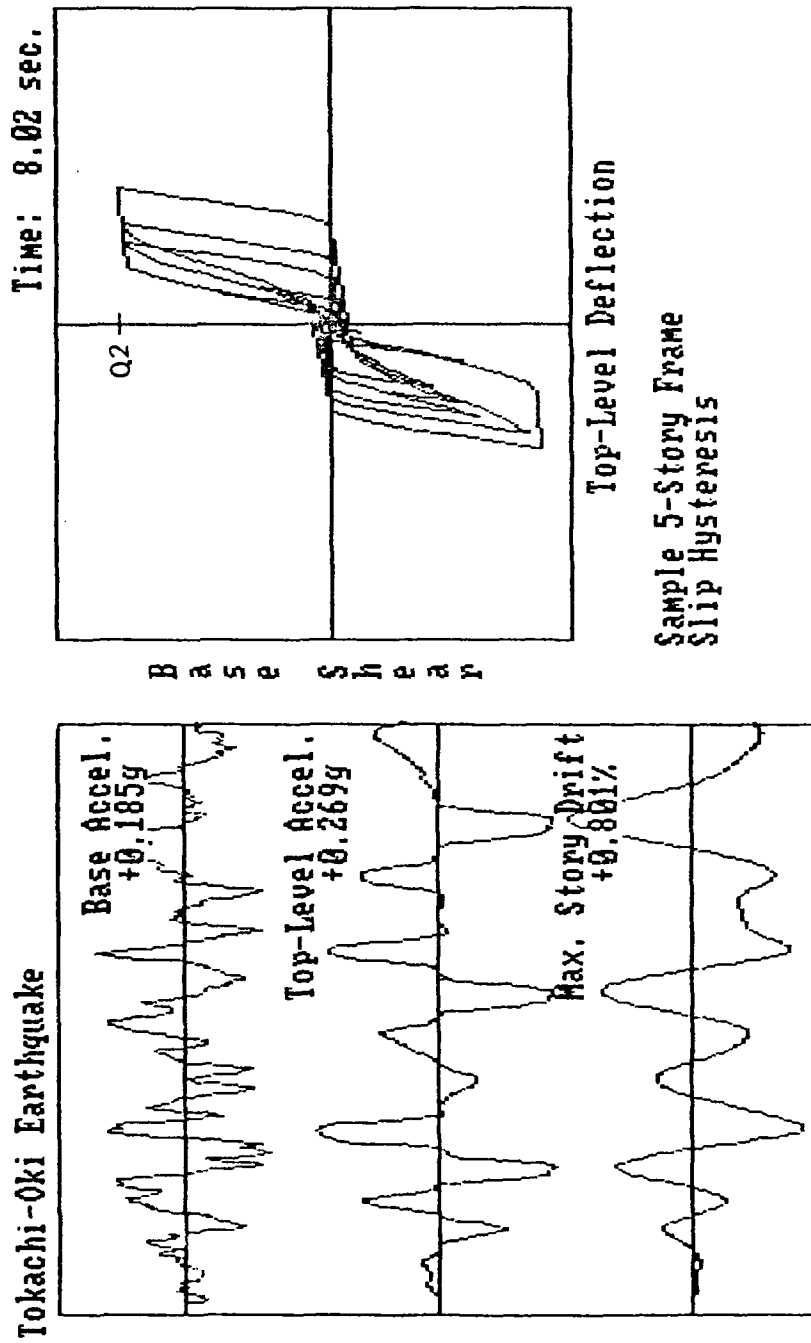


Fig. 6.3a Computed Response to Tokachi-Oki

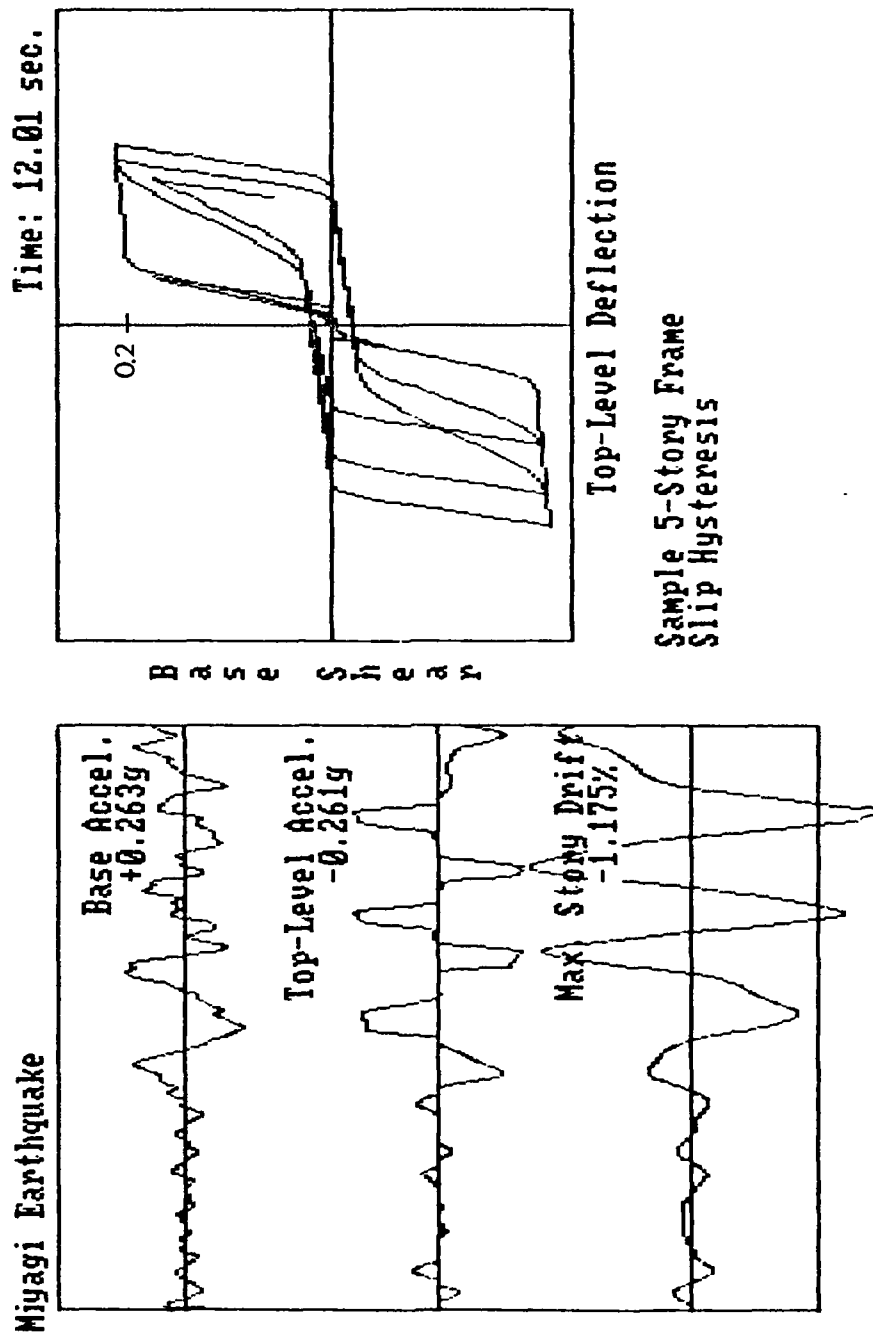


Fig. 6.3b Computed Response to Miyagi

Imperial Valley Earthquake - May 18 1940 - El Centro - NS Time: 8.01 sec.

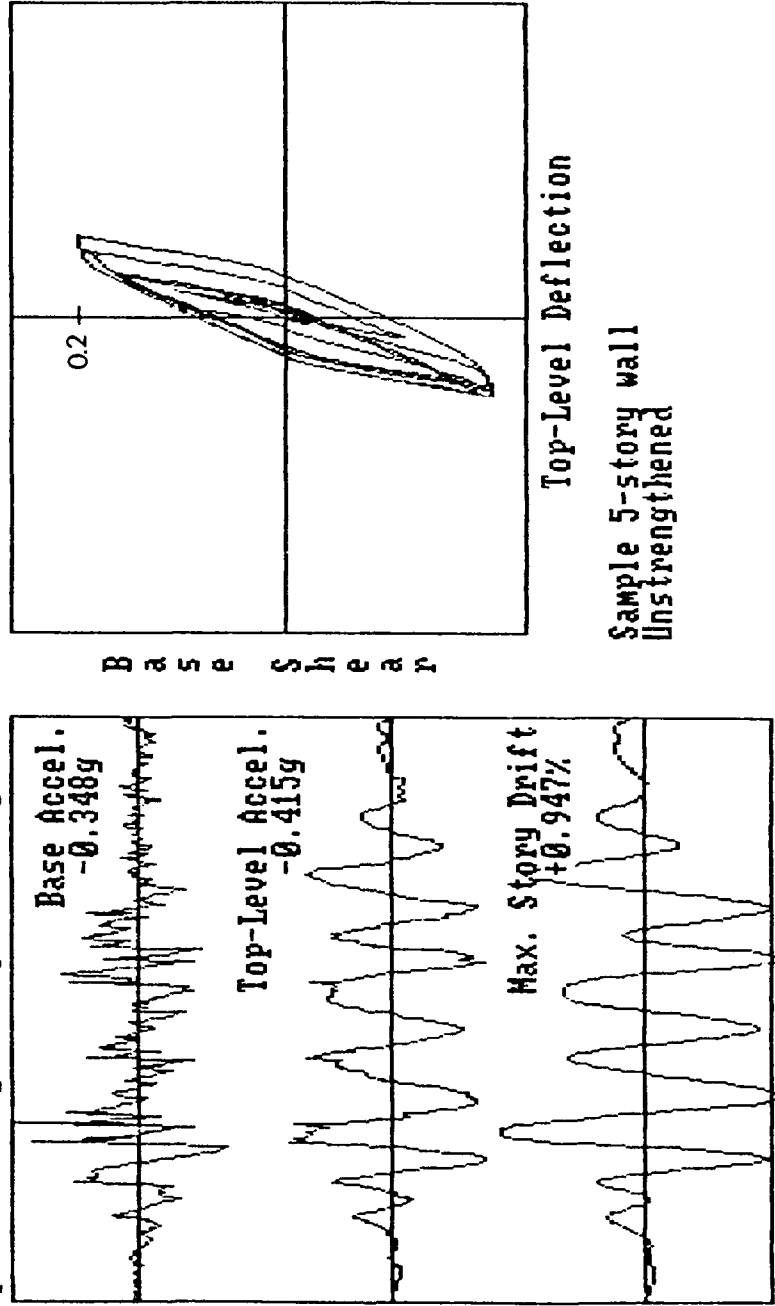


Fig. 6.4a Computed Response of Unstrengthened Structure

Imperial Valley Earthquake - May 18 1940 - El Centro - NS Time: 8.02 sec.

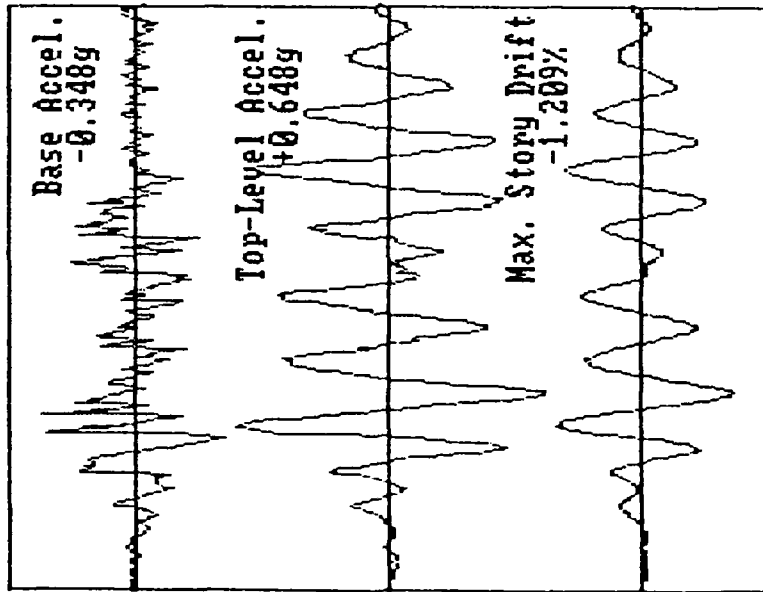
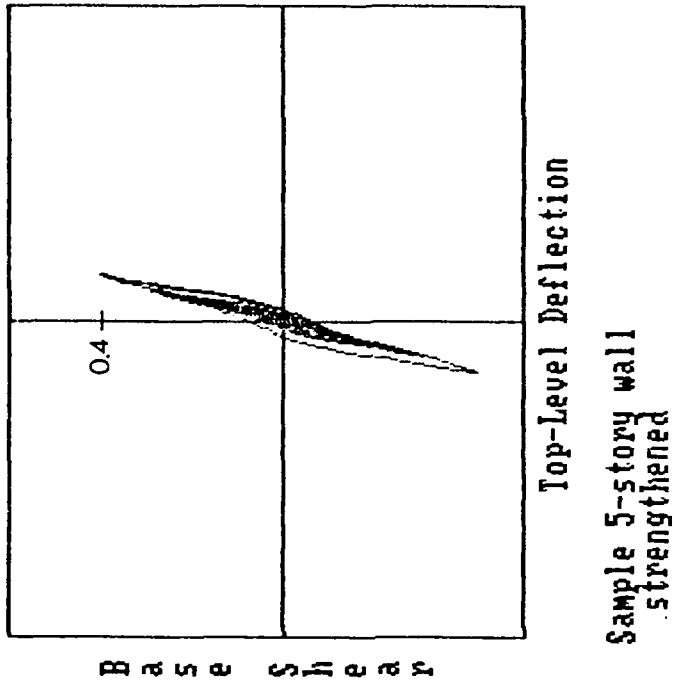


Fig. 6.4b Computed Response of Strengthened Structure

7.0 Future Development

The study described in this report represented an initial effort which was primarily concerned with development of suitable algorithms for nonlinear response and programming of the algorithms for use in an interactive mode. Future work should be directed towards verification and sensitivity studies using the computational models. Such studies may include comparison of results with that of more detailed multi-degree-of-freedom models. The generalized hysteresis formulation should be checked with experimental data from laboratory experiments, and changed accordingly. Sensitivity studies may investigate the dependence of the computed response on different hysteresis modeling assumptions, or to different base motions. The library of recorded motions could be increased.

Further development of the numerical model may consist of adding a degree of freedom so that both lateral and torsional motions of unsymmetrical structures could be analysed. A two-degree-of-freedom model would still be appropriate for computation on a microcomputer.

8.0 References

1. NAVFAC P-355 AND P-355.1 Technical Manuals: Seismic Design for Buildings.
2. Tentative Provisions for the Development of Seismic Regulations for Buildings, Applied Technology Council, ATC-03, National Bureau of Standards SP-510, 1978.
3. Abrams, D.P., and M.A. Sozen, "Experimental Study of Frame-Wall Interaction in Reinforced Concrete Structures Subjected to Strong Earthquake Motions," Civil Engineering Studies, Structural Research Series Report No. 460, University of Illinois, Urbana, May 1979.
4. Seismic Resistance of Reinforced Concrete Shear Walls and Frame Joints: Implications of Recent Research for Design Engineers, Applied Technology Council, ATC-11.
5. Inelastic Response of Concrete Structures, future special publication of American Concrete Institute, Ad-hoc committee report of ASCE-ACI Committee 442: Response of Concrete Buildings to Lateral Forces.
6. Earthquake Effects on Reinforced Concrete Structures - U.S.-Japan Research, Special Publication of American Concrete Institute, SP-84, 1985.
7. Clough, R.W., and J. Penzien, Dynamics of Structures, First Edition, McGraw-Hill, 1975, Chapter 7.
8. Newmark, N.M., "A Method of Computation for Structural Dynamics," Journal of the Engineering Mechanics Division, ASCE, Vol. 85, No. EM 3, July 1959.
9. Newmark, N.M., and W.J. Hall, "Procedures and Criteria for Earthquake Resistant Design," Proceedings of National Workshop on Building Practices for Disaster Mitigation, U.S. Department of Commerce, National Bureau of Standards, 1972.
10. Lai, S.P., and J.M. Biggs, "Inelastic Response Spectra for Aseismic Building Design," Journal of the Structural Division, ASCE, Vol. 106, No. ST6, June 1980.

11. Riddell, R., and N.M. Newmark,, "Statistical Analysis of the Response of Nonlinear Systems Subjected to Earthquakes," Civil Engineering Studies, Structural Research Series Report No. 468, University of Illinois, Urbana, August 1979.
12. Mahin, S.A., and J. Lin, "Construction of Inelastic Spectra for Single-Degree-of-Freedom Systems," Report No. UCB/EERC-83/17, Earthquake Engineering Research Center, University of California, Berkeley, June 1983.
13. Mahin, S.A., and V.V. Bertero, "An Evaluation of Inelastic Design Spectra," Journal of the Structural Division, ASCE, Vol. 107, No ST9, September 1981.
14. Saiidi, M., and M.A. Sozen, "Simple Nonlinear Seismic Analysis of R/C Structures," Journal of the Structural Division, ASCE, Vol. 107, No. ST5, May 1981.
15. Clough, R.W., and S.B. Johnson, "Effect of Stiffness Degradation on Earthquake Ductility Requirements," Proceedings of the Second Japan Earthquake Engineering Symposium, pp. 227-232, 1966.
16. Takeda, T.M., M.A. Sozen, and N.N. Neilson, "Reinforced Concrete Response to Simulated Earthquakes," Journal of the Structural Division, ASCE, Vol. 96, No. ST12, 1970.
17. Abrams, D.P., and S. Tangkijngamvong, "Dynamic Response of Reduced-Scale Models and Reinforced Concrete Structures," Proceedings of the Eighth World Conference on Earthquake Engineering, San Francisco, CA, July 1984, Vol. VI, pp.371-378.
18. Lew, T.K., and S.K. Takahashi, "Rapid Seismic Analysis Procedure," Technical Memorandum No. 51-78-02, Naval Civil Engineering Laboratory, April 1978.
19. Lew, T.K., "Modifications for Enchancing the Rapid Seismic Analysis Procedure," Technical Memorandum No. 51-83-07, Naval Civil Engineering Laboratory, April 1983.

APPENDIX A MANUAL FOR PROGRAM USAGE

Introductory information

The computer program "NEABS" computes response of a nonlinear, single-degree-of-freedom oscillator to a specified earthquake motion.

The program may run on an IBM PC, XT or AT, or compatible equipment with a single disk drive. The source program is written in GW Basic 2.0 which is consistent with the Microsoft MS-DOS operating system.

To run the program, insert the program disk and type the following three statements.

- (a) A> BASICA
- (b) LOAD "NEABS"
- (c) RUN

Initially, the user is introduced to the function of the program with a display of introductory remarks (Fig. A.1). To start the input session, press the right arrow key.

Input information

The user provides the following information to the program during an interactive session.

- (a) the mass distribution
- (b) a selection of assumed deflected shape
- (c) a construction of the hysteretic relation between the ratios of base shear and weight (lateral force coefficient), and top-level deflection and height (percent drift).
- (d) a selection of the earthquake motion

Descriptions of each set of input information are described below.

Mass distribution

The mass distribution is defined in terms of the relative weights of each story level. The total weight of the structure is unimportant and not necessary because the resistance is expressed in terms of the ratio of strength to weight.

If all story weights are the same, a simple "yes" is a sufficient reply to a prompt provided by the program. If story weights are variable, the user is prompted to specify individual weights per level. If all story heights are the same, again, a simple "yes" is sufficient in addition to a numerical value for the typical story height. If story heights are variable, the user is prompted for the height of each story. A display will be given of this input information for user verification after the deflected shape is selected.

Deflected shape

A deflected shape must be prescribed so that internal forces of each story mass may be condensed to a single generalized mass. The generalized coordinate considered by the program is the lateral displacement at the top level. The assumed deflected shape is also used to transform the hysteretic force-deflection relation in terms of the generalized coordinate.

One of three shapes may be selected: a parabolic flexure beam (wall structures), a triangle (frame-wall structures), or a parabolic shear beam (frame structures). Options may be scanned using the up and down arrow keys, and selected using the right arrow key.

Following this input, a display (Fig. A.2) is shown on the screen for verification of the mass distribution, and the prescribed deflected shape. In addition, the following normalization factors are presented for the chosen mass distribution.

$$\alpha = \{\phi\}^t [M] \{1\} / \{\phi\}^t [M] \{\phi\}$$

$$\beta = \{1\}^t [M] \{1\} / \{1\}^t [M] \{\phi\}$$

[M] is the mass matrix, and $\{\phi\}$ is the prescribed deflected shape. The first term is commonly referred to as the modal participation factor and is used to scale the base accelerations. The second term is multiplied times the resisting force to transform it to the modal coordinates.

To continue the input session, press the right arrow key.

Hysteretic force-deflection relation

The force resisted by the structure is represented in terms of the ratio of base shear to total weight. Lateral deflections are represented with the ratio of top-level deflection to total height, or the percentage of drift for the overall structure. Stiffness of the structure must be expressed in terms of the ratio of these normalized values.

Input information which is requested interactively with screen displays consists of the following parameters for each direction of loading.

(a) A linear strength envelope (Fig. A.3a). The user specifies an intercept value on the ordinate axis and a slope. Base-shear strength may be determined by considering a hinge mechanism for the structure, and using virtual work with an assumed distribution of lateral force. For a more approximate analysis, base shear capacity may be estimated from an equivalent base shear coefficient, or the sum of cross-sectional areas of members at the base story.

(b) Percentage of lateral drift resulting in formation of mechanism for first inelastic cycle (Fig. A.3b). The algorithm uses this value to

define the elastic stiffness, and thus the fundamental period of vibration and the maximum time step to be used for the computations. Because the stiffness is modeled with deterioration, this deflection value represents only that for cycles prior to the first inelastic excursion. Estimates of this deflection may be obtained from an static elastic analysis, or more approximately, from an estimate of the fundamental period.

(c) Unloading slope (Fig. A.3c). Units of this value should reflect the nondimensionality of the force and deflection. The algorithm considers this value to be a constant for all cycles.

(d) Force-reversal slope (Fig. A.3d). This slope represents the reduction in stiffness after the force is reversed and before the structure stiffens. For a member analysis, it would represent the condition of crack closure, and could be modeled with a section comprised solely of tensile and compressive reinforcement. For a building analysis, the slope in this range can be determined from a nonlinear static analysis where the members are modeled with this characteristic. Otherwise, the value for this stiffness is somewhat subjective. However, because energy dissipation is small in this range of loading, response is usually not sensitive to this stiffness value. If the structure is comprised of mostly frames, a suitable approximation is 5 to 10% of the loading slope. If the structure is comprised of walls, this value can be approximated with 30 to 40% of the loading slope. It may be worthwhile to run a few analyses varying this stiffness because an accurate representation is often not possible.

The algorithm decreases the reversal stiffness as new maximum deflections during the previous cycle have been reached. This model represents bond deterioration in the compressive reinforcement.

Through proper selection of these parameters, nearly any hysteretic relation can be constructed including elasto-plastic, stiffness degrading, and softening behavior upon reversal of force.

The user may check the chosen hysteretic formulation before computing response histories by responding "yes" to the prompt, and then controlling the direction of lateral deflection with the right and left arrows on the keyboard (Fig. A.3e). This is an illustrative exercise to study the intricacies implicit in the program for generation of the force-deflection relation for any particular deflection history. To return to the input session, press the down arrow key.

Earthquake motion

A menu of several recorded earthquake motions is shown on the screen (Fig. A.4f). The user scans the menu using the up and down arrows, and makes a selection using the right arrow. The user then is requested to specify the duration and the maximum acceleration of the motion that is to be used for the computation. The time axis of the motion may be scaled as well if response to simulated earthquake motions is of interest.

Plots of each recorded accelerogram as stored on disk are provided in Appendix C.

Output

Output consists of response histories of lateral absolute acceleration at the top level, and lateral drifts at the critical story (Fig. A.5). In addition, the relation between normalized base shear and top-level deflection is plotted to show the history of structural resistance. Data is displayed on the screen as the computation progresses. Numerical values for response are shown for each instant.

A beep sounds to alert the user when the computation is done. Values for response maxima are shown on the screen. At that time, screen information may be dumped to a printing device by pressing the "prt sc" key. The sequence is concluded with a request for future processing. The user may select to redefine the earthquake motion, the hysteresis formulation, to start again, or to stop.

To return to the operating system from BASIC, type "SYSTEM."

This program computes nonlinear dynamic response of building systems that may be characterized solely with their fundamental mode of response.

Required input information consists of:

- (a) mass distribution
- (b) form of lateral deflected shape
- (c) ratio of base-shear capacity to building weight
- (d) overall stiffness in terms of ratio of top-level deflection to height
- (e) selection of hysteresis formulation
- (f) selection of earthquake motion

Output information consists of:

- (a) response histories of acceleration and lateral deflection
- (b) nonlinear force-deflection relation

Please follow along.....

Press right arrow to continue

Fig. A.1 Introductory Remarks

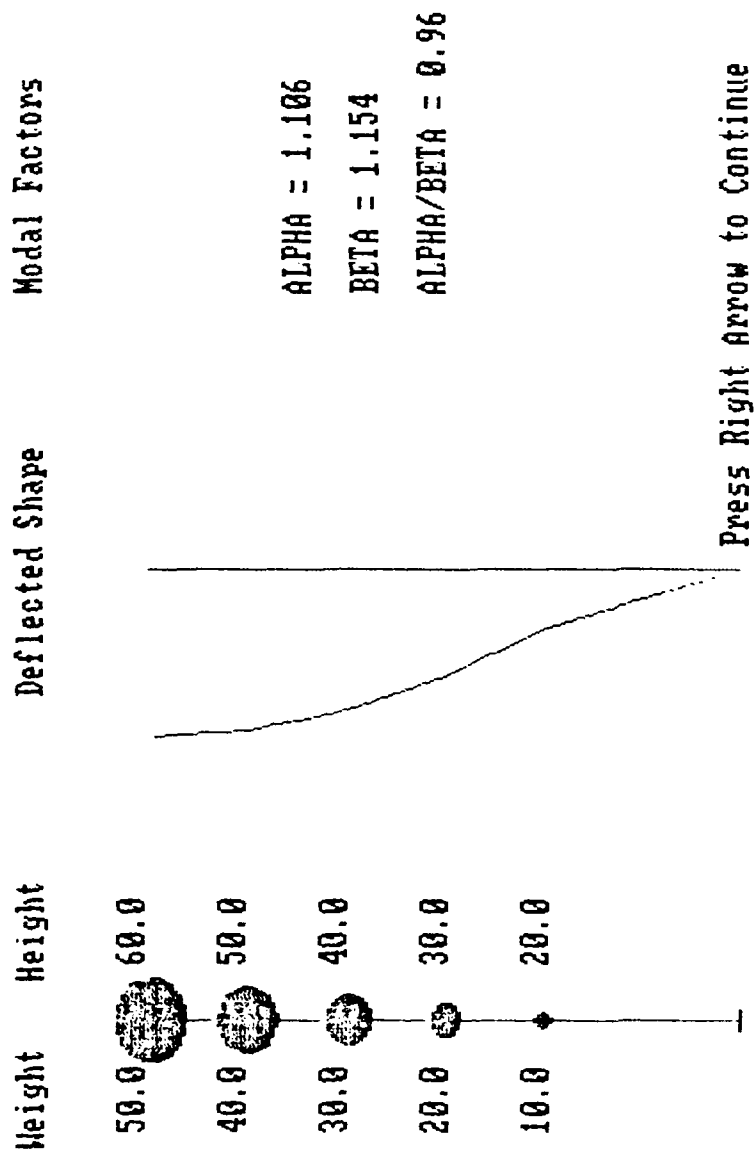


Fig. A.2 Verification of Mass Distribution

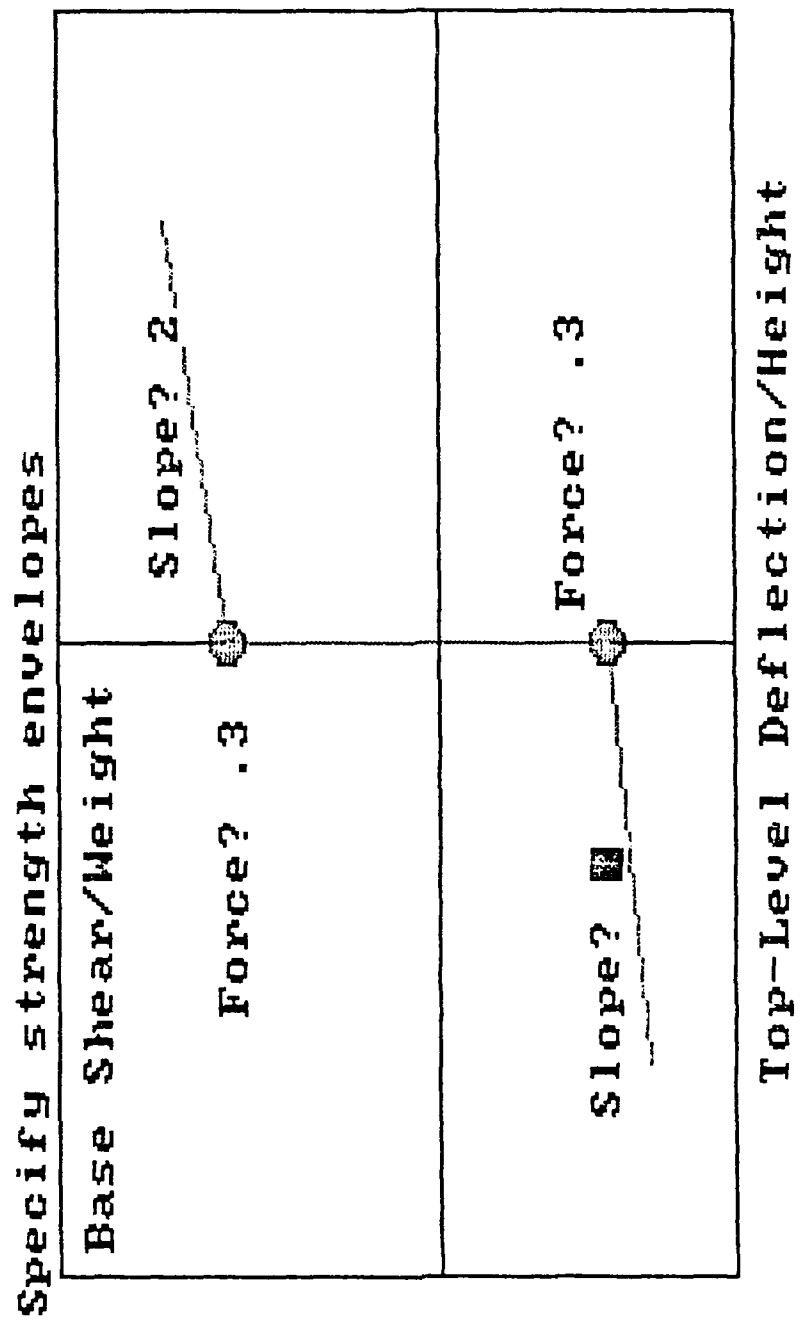
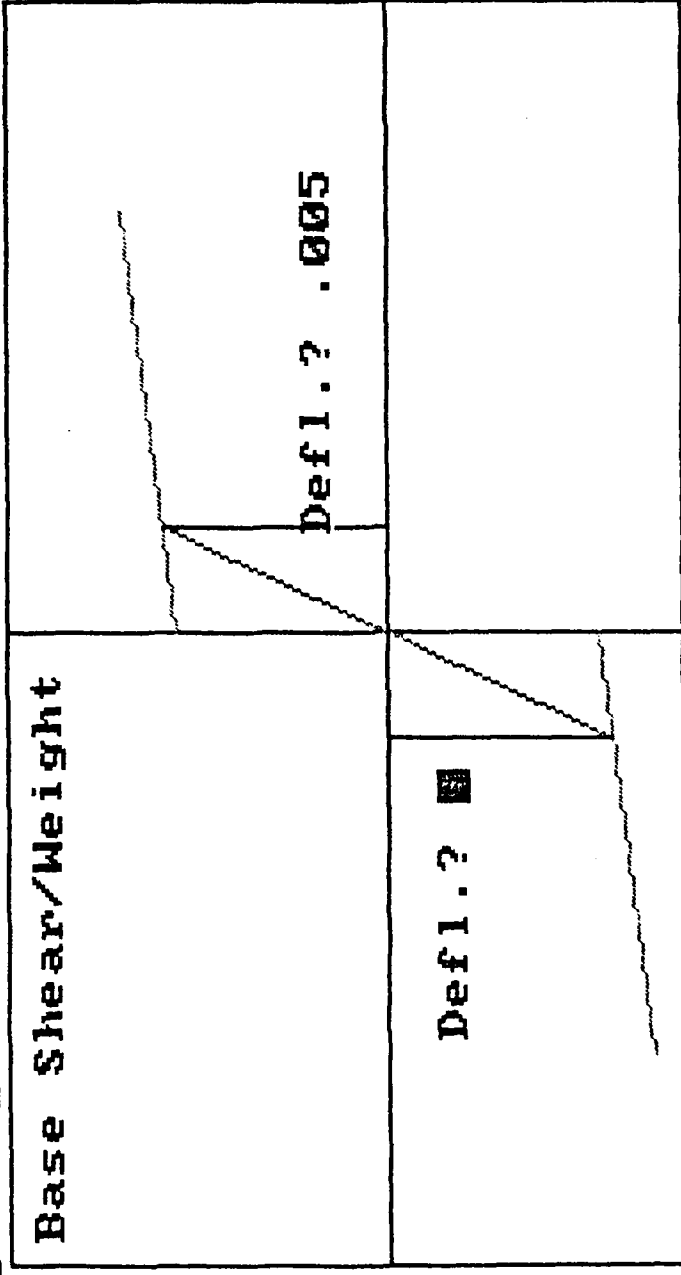


Fig. A.3a Strength Envelopes

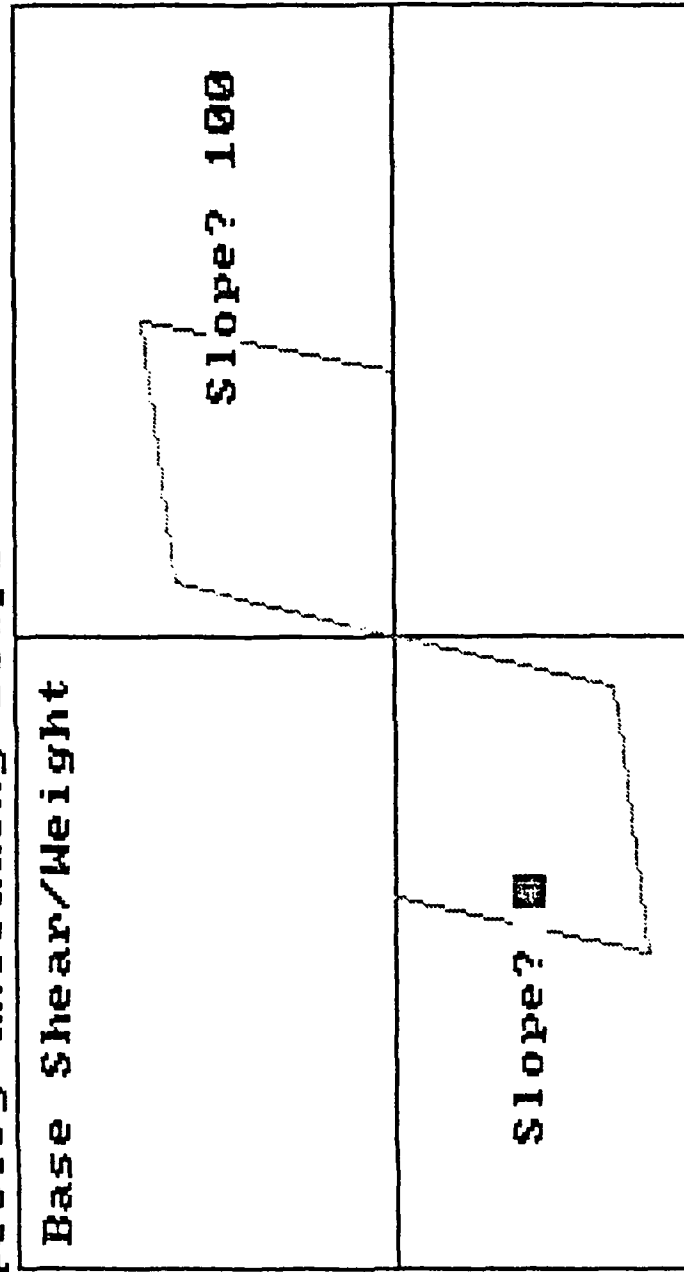
Specify yield deflections



Top-Level Deflection/Height

Fig. A.3b Deflections at First Inelastic Range

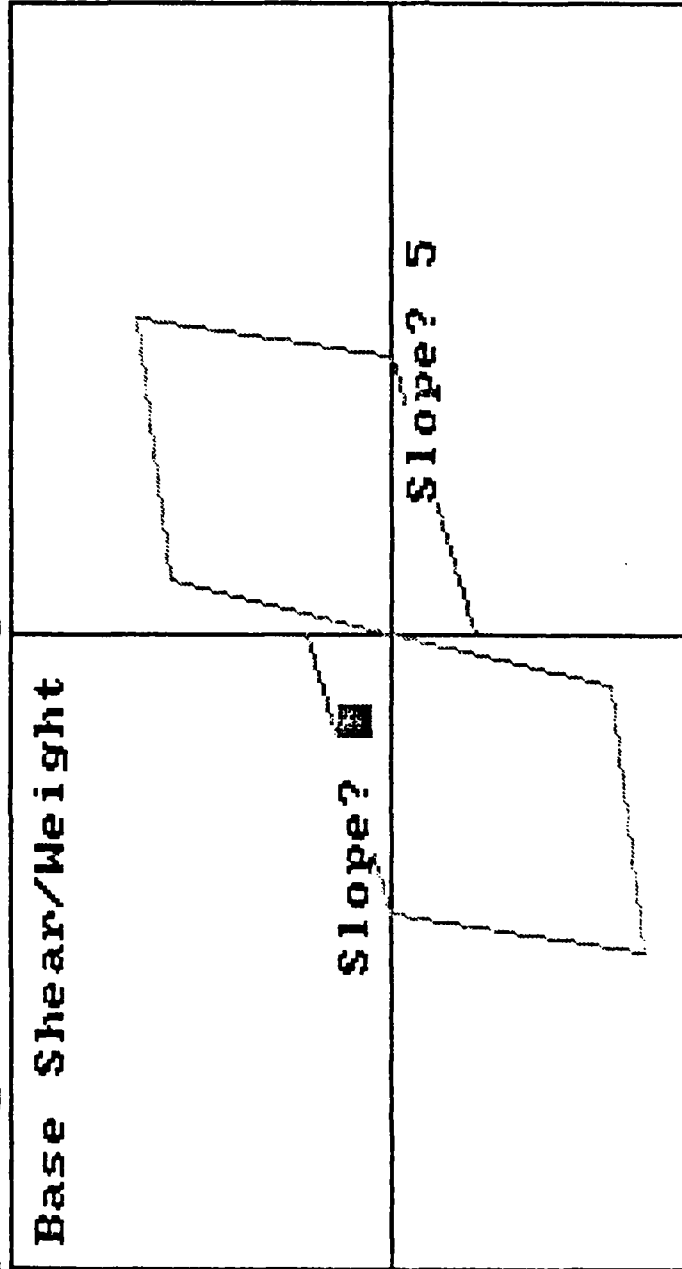
Specify unloading slopes



Top-Level Deflection/Height

Fig. A.3c Unloading Slopes

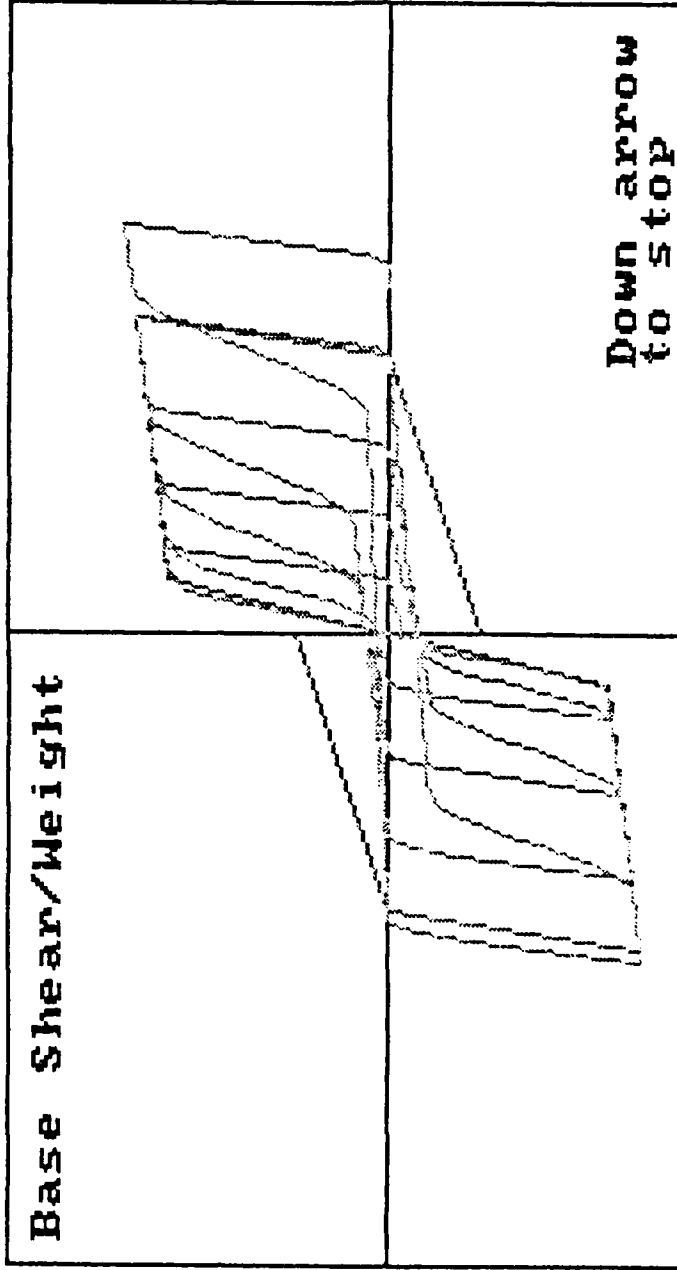
Specify reversal slopes



Top-Level Deflection/Height

Fig. A.3d Force-Reversal Slopes

Use arrows to change direction



Top-Level Deflection/Height

Select a motion

Scan options using up and down arrows
Make selection with right arrow

Imperial Valley Earthquake - May 18 1940 - El Centro - NS

San Fernando Earthquake - Feb 9 1971 - Pacoima Dam - S16E

San Fernando Earthquake - Feb 9 1971 - Castaic Old Ridge Route - N21E

San Fernando Earthquake - Feb 9 1971 - 3710 Wilshire Blvd. 10th Fl. - N90E

Parkfield Earthquake - June 27 1966 - Temblor - S25W

Kern Co. Earthquake - July 21, 1952 - Santa Barbara Courthouse - S48E

Parkfield Earthquake - June 27 1966 - Cholame, Shandon - N85E

Miyagi Earthquake

Tokachi-Oki Earthquake

Fig. A.4 Menu of Earthquake Motions

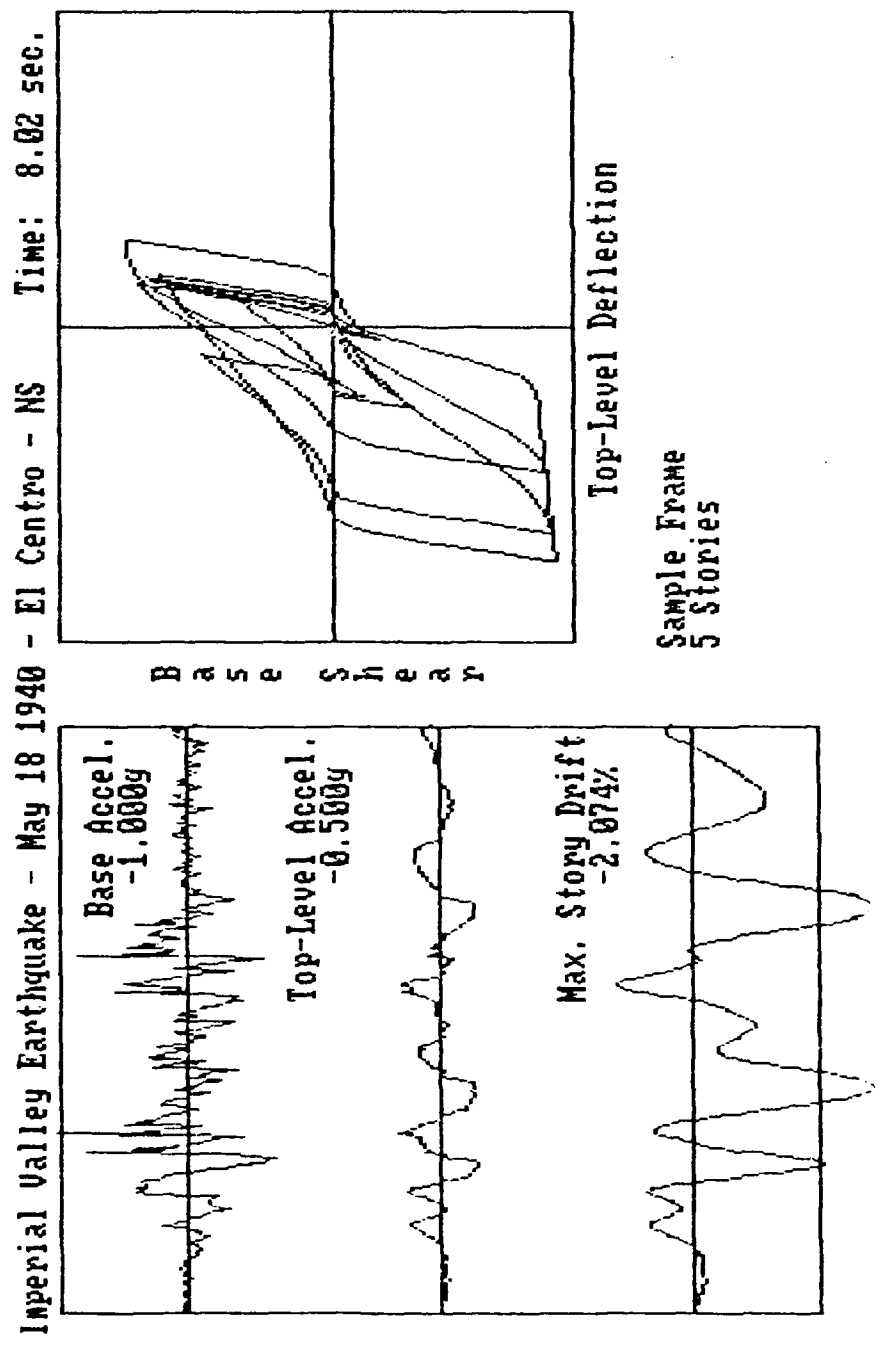


Fig. A.5 Sample Output

APPENDIX B PROGRAM LISTING

```

1  REM      "Nonlinear Earthquake Analysis of Building Systems"
2  REM      "NEABS"
3  REM      This program computes nonlinear response of building
4  REM      structures to earthquake motions.
5  REM
10 DIM D(1200),V(1200),A(1200),P(1200),T(2000),R(1200),C$(10)
17 REM
18 REM      Call subroutines
19 REM
20 GOSUB 4000      'Specify mass distribution and deflected shape'
21 GOSUB 2500      'Specify hysteresis'
22 GOSUB 2000      'Check hysteresis'
23 GOSUB 3000      'Select earthquake motion'
24 GOSUB 1000      'Plot screen format for output response'
25 REM
26 REM
28 DMAX=5*XYP: RMAX=1.1*(BP+5*KCP*XYP)      'sets plotting scales'
29 REM      Determine fund. period for damping and time step
30      KP=BP/XYP+KCP: G=32.2: W=(BETA*G*KP/TH)^.5: C=2*W*C: T1=6.28319/W
31      TSTEP=TSTEP/TSCALE: DUR=DUR/TSCALE
32      H=.1*T1: H1=TSTEP: IF H>H1 THEN H=H1
33 REM      Factor base accelerations
34      P3=0: P4=(-1)*P4*ALPHA: M=1
180 REM
181 REM      Time step integration
182 REM
185      VTOL=.01*XYP*W
207      J=0: L=1: D2=0: V2=0: D4MAX=0: A4MAX=0
208      DMP=XYP: DMN=XYN: XMN=XYN: YMN=0: XMP=0: YMP=0
209      KAVP=BP/XYP+KCP: KABP=KAVP: KAVN=BN/XYN+KCN: KABN=KAVN
211      A2=P4 : LOCATE 23,50: PRINT ".."
215      IF P4>0 THEN Z=1: XM=0: YM=0: XA=0: YA=0: XB=0: YB=0: XC=XYP: YC=BP+K
CP*XC: KB=YC/XC: KC=KCP: B=BP: GOTO 399
216      IF P4<0 THEN Z=-1: XM=0: YM=0: XA=0: YA=0: XB=0: YB=0: XC=XYN: YC=BN+
KCN*XC: KB=YC/XC: KC=KCN: B=BN: GOTO 399
218 REM
219 REM      Intialize variables for new path at change in sign of velocity
220 REM
221      H=H1
222      IF XMN<DMN THEN DMN=XMN: IF ZA=1 THEN KAEN=KAVN
223      IF XMP>DMP THEN DMP=XMP: IF ZA=1 THEN KABP=KAVP
225      IF Z=-1 THEN 270
230      IF YMN>0 THEN ZA=3: XM=XMN: YM=YMN: YA=YMP-YM: KA=KAP: XA=YA/KA: XB=X
A: YB=YA: KB=SLP: B=BP: XC=DMP-XM: KC=KCP: YC=KC*DMP+B-YM: GOTO 390
235      ZA=1: XM=XMN: YM=YMN: KA=KAN: KBO=KEP: X9=DMP: B=BP: DBL=DELP: XC1=DMP:
KC=KCP: KAV=KABP
236      GOTO 330
270      IF YMP<0 THEN ZA=3: XM=XMP: YM=YMP: YA=YMN-YM: KA=KAN: XA=YA/KA: XB=X
A: YB=YA: KB=SLN: B=BN: XC=DMN-XM: KC=KCN: YC=KC*DMN+B-YM: GOTO 390
280      ZA=1: XM=XMP: YM=YMP: KA=KAP: KBO=KBN: X9=DMN: B=BN: DBL=DBLN: XC1=DMN:
KC=KCN: KAV=KAEN
327 REM
328 REM      Compute cubic splines
329 REM
330      IF X9/DBL>1 THEN KB=0: SET1=1!: GOTO 340

```

```

340 YA=-YM: XA=YA/KA: XB=BET1*(-XM-XA)-XM: YB=KB*(XB-XA)+YA
341 IF XB*Z<XA*Z THEN XB=XA: YB=YA: KB=KAV: ZA=2
342 XC=XC1-XM: YC=KC*XC1+B-YM
350 IF ZA=1 AND (YC-YB)/(XC-XB)>KAV, THEN XC=(KAV*XB+B+KC*XM-YB-YM)/(KAV-
KC): YC=KAV*(XC-XB)+YB
360 IF ZA=1 AND KB>(YC-YA)/(XC-XA) THEN XB=XA: YB=YA
380 IF XA=0 THEN 399
390 AA=(KA*XA+KB*XA-2*YA)/XA^3: BA=(3*YA-KB*XA-2*KA*XA)/XA^2
399 LX=XC-XB: LY=YC-YB: AB=(KB*LX+KC*LX-2*LY)/LX^3: BB=(3*LY-KC*LX-2*KB*LX)
/LX^2
401 REM
402 REM Follow path for each time step H until zero velocity is reached
403 REM
410 J=J+1: D1=D2: V1=V2: A1=A2: IF J=1 THEN A1=0: LOCATE 23,51+J: PRINT ".."
412 V2=V1+(A1+A2)*H/2
414 D2=D1+(V1*H+A1*H^2/3+A2*H^2/6)*G/TH
419 IF Z=1 AND V2<(-1)*VTOL THEN H=H/2: GOTO 412
420 IF Z=-1 AND V2>VTOL THEN H=H/2: GOTO 412
430 REM
431 REM Determine resisting force for particular deflection
432 REM
433 X=D2-XM
435 IF X*Z<XA*Z THEN Y=AA*X^3+BA*X^2+KA*X: SL=3*AA*X^2+2*BA*X+KA
436 IF X*Z>XA*Z AND X<XB*Z, THEN Y=YA+KB*(X-XA): SL=KB
438 IF X*Z>XB*Z AND X<XC*Z, THEN X0=X-XB: Y=YB+AB*X0^3+BB*X0^2+KB*X0: SL
=3*AB*X0^2+2*BB*X0+KB
440 IF X*Z>XC*Z THEN Y=YC+KC*(X-XC): SL=KC
445 IF (Y+YM)*Z>((X+XM)*KC+B)*Z THEN Y=-YM+(X+XM)*KC+B
450 R2=Y+YM
505 P2=P3+(P4-P3)*(T(J-1)+H-(L-1)*H1)/H1
506 B2=(P2-C*V2-BETA*R2)/M
510 IF ABS((B2-A2)/A2)>.02, THEN A2=B2: GOTO 412
511 REM
512 REM Process information for time step
513 REM
515 A4=A2-P2/ALPHA: D4=D2*ISDEF
520 IF ABS(D4)>ABS(D4MAX) THEN D4MAX=D4
521 IF ABS(A4)>ABS(A4MAX) THEN A4MAX=A4
586 D(J)=D2: V(J)=V2: A(J)=A4: R(J)=R2: T(J)=T(J-1)+H
588 X1=X2: X2=T(J)*280/DUR+10
590 Y1=Y2: Y2=40-(P2/ALPHA)*20/AMAX: LINE (X1,Y1)-(X2,Y2),3
591 Y3=Y4: Y4=100-A4*20/AMAX: LINE (X1,Y3)-(X2,Y4),3
592 Y5=Y6: Y6=160-D4*60/DMAX: LINE (X1,Y5)-(X2,Y6),3
594 X7=X8: X8=480+D2*145/DMAX: Y7=Y8: Y8=75-R2*60/RMAX: LINE (X7,Y7)-(X8
,Y8),3
595 IF J=1 THEN LOCATE 1,63: PRINT "Time: sec.": LOCATE 23,44: P
RINT "
596 LOCATE 1,69: PRINT USING "##.##";T(J)
598 LOCATE 4,28: PRINT USING "+#.###g";(-1)*P2/ALPHA: LOCATE 10,28: PRIN
T USING "+#.###g";A4: LOCATE 18,28: PRINT USING "+#.###%";D4*100
610 IF T(J)>L*H1 AND T(J)<DUR THEN L=L+1: P3=P4: INPUT #1, P4: P4=(-1
)*ALPHA*P4*AMAX/AMAX1
615 IF T(J)>=DUR THEN 699
630 IF Z=-1 THEN 650
640 IF V2<0 AND V2>-VTOL, THEN Z=-1: XMP=D1: YMP=R2: SLP=SL: KAVP=(YC-
YB)/(XC-XB): GOTO 220
645 GOTO 410
650 IF V2>0 AND V2<VTOL, THEN Z=1: XMN=D1: YMN=R2: SLN=SL: KAVN=(YC-YB
)/(XC-XB): GOTO 220
660 GOTO 410
699 NJ=J: CLOSE #1
700 LOCATE 4,28: PRINT USING "+#.###g";AMAX: LOCATE 10,28: PRINT USING "+#.###
g";A4MAX: LOCATE 18,28: PRINT USING "+#.###%";D4MAX*100
710 PLAY "ABA": FOR I=1 TO 3: LOCATE 23,42: PRINT "COPY..Press Shift Prt Sc":
FOR J=1 TO 700: NEXT J: LOCATE 23,42: PRINT " ": FOR J=1

```

```

715 LOCATE 19,42: PRINT "Select variable for next computation": LOCATE 20,42:
PRINT " Use right and left arrows to scan "
716 LOCATE 21,42: PRINT " Press down arrow to select "
720 B$(1)="EQKE": B$(2)="HYSTR": B$(3)="START": B$(4)="STOP"
730 X=43: FOR J=1 TO 4: LOCATE 23,X: PRINT B$(J): X=X+10: NEXT J
740 X=330: FOR I=1 TO 4: LINE (X,170)-(X+48,190),3,B: X=X+80: NEXT I
750 J1=1: J=0
760 A$=INKEY$:IF A$="" THEN 760
770 A$=RIGHT$(A$,1)
780 IF A$="M" THEN J=J+1
790 IF A$="K" THEN J=J-1
800 IF A$="P" THEN 898
810 IF J1=1 THEN 830
820 LINE (X1,170)-(X1+48,190),0,BF: LINE (X1,170)-(X1+48,190),3,B: LOCATE 23,4
3+10*(L-1): PRINT B$(L): X=330+80*(J-1): LINE (X,170)-(X+48,190),3,BF: X1=X: L=J
: GOTO 760
830 X=330+80*(J-1): LINE (X,170)-(X+48,190),3,BF: X1=X: L=J: J1=2: GOTO 760
898 ON J GOTO 23,21,20,899
899 CLS: END
998 REM
999 REM
1000 REM
1001 REM This subroutine sets screen format for response history display
1002 REM
1036 CLS: SCREEN 2,0,0: KEY OFF
1038 LINE (10,10)-(290,190),3,B: LINE (10,40)-(290,40),3: LINE (10,100)-(290,10
0),3: LINE (10,160)-(290,160),3
1040 LINE (330,10)-(630,132),3,B: LINE (330,75)-(630,75),3: LINE (480,10)-(480,
132),3
1042 LOCATE 1,1: PRINT A$
1045 LOCATE 3,26: PRINT "Base Accel.": LOCATE 9,21: PRINT "Top-Level Accel.": LO
CATE 17,21: PRINT "Max. Story Drift"
1046 LOCATE 18,51: PRINT "Top-Level Deflection": A$(1)="B": A$(2)="a": A$(3)="s"
: A$(4)="e": A$(5)=" ": A$(6)="S": A$(7)="h": A$(8)="e": A$(9)="a": A$(10)="r":
FOR I=1 TO 10: LOCATE I+4,40: PRINT A$(I): NEXT I
1048 LOCATE 20,42: PRINT NOTE1$: LOCATE 21,42: PRINT NOTE2$
1049 LOCATE 23,44: PRINT "WAIT.."
1050 X2=10: Y2=40: Y4=100: Y6=160: Y8=75: X8=480
1060 RETURN
2000 REM
2001 REM
2002 REM This program allows the user to study or check a hysteresis
2003 REM formulation. The left and right arrows on the keyboard are
2004 REM used to change the direction of loading (rather than a change in
2005 REM sign of velocity as computed by the main program). Note that the
2006 REM remainder of the subroutine is nearly identical to the code in the
2007 REM main part of the program.
2008 REM
2020 LOCATE 1,1: PRINT "Use arrows to change direction "
2021 LOCATE 20,29: PRINT "Down arrow": LOCATE 21,29: PRINT "to stop"
2042 LINE -(160,100),3
2208 D2=0: Z=1: DMP=XYP: DMN=XYN: XMN=XYN: YMN=0: XMP=0: YMP=0
2210 KAVP=BP/XYP+KCP: KABP=KAVP: KAVN=BN/XYN+KCN: KABN=KAVN
2215 XM=0: YM=0: XA=0: YA=0: XB=0: YB=0: XC=XYP: YC=BP+KCP*XC: KB=YC/XC: KC=KCP:
B=BP: GOTO 2399
2218 REM
2219 REM Intialize variables for new path at change in sign of velocity
2220 REM
2222 IF XMN<DMN THEN DMN=XMN: IF ZA=1 THEN KABN=KAVN
2223 IF XMP>DMP THEN DMP=XMP: IF ZA=1 THEN KABP=KAVP
2225 IF Z=-1 THEN 2270
2230 IF YMN>0 THEN ZA=3: XM=XMN: YM=YMN: YA=YMP-YM: KA=KAP: XA=YA/KA: XB=
XA: YB=YA: KB=SLP: B=BP: XC=DMP-XM: KC=KCP: YC=KC*DMP+B-YM: GOTO 2390
2235 ZA=1: XM=XMN: YM=YMN: KA=KAN: KEO=KBP: X9=DMP: S=BP: DBL=DBLP: XC1=DMP
: KC=KCP: KAV=KABP

```

```

2270      IF YMP<0 THEN ZA=3: XM=XMP: YM=YMP: YA=YMN-YM: KA=KAN: XA=YA/KA: XB=
XA: YB=YA: KB=SLN: B=BN: XC=DMN-XM: KC=KCN: YC=KC*DMN+B-YM: GOTO 2390
2280      ZA=1: XM=XMP: YM=YMP: KA=KAP: KBO=KBN: X9=DMN: B=BN: DBL=DBLN: XC1=DMN
: KC=KCN: KAV=KABN
2327 REM
2328 REM      Compute cubic splines
2329 REM
2330      IF X9/DBL>1 THEN KB=0: BET1=1!: GOTO 2340
2335      BET1=X9/DBL: KB=KBO*(1-X9/DBL)^1.5
2340      YA=-YM: XA=YA/KA: XB=BET1*(-XM-XA)-XM: YB=KB*(XB-XA)+YA
2341      IF XB*Z<XA*Z THEN XB=XA: YB=YA: KB=KAV: ZA=2
2342      XC=XC1-XM: YC=KC*XC1+B-YM
2350      IF ZA=1 AND (YC-YB)/(XC-XB)>KAV, THEN XC=(KAV*XB+B+KC*XM-YB-YM)/(KAV
-KC): YC=KAV*(XC-XB)+YB
2360      IF ZA=1 AND KB>(YC-YA)/(XC-XA), THEN XB=XA: YB=YA
2380      IF XA=0 THEN 2399
2390      AA=(KA*XA+KB*XA-2*YA)/XA^3: BA=(3*YA-KB*XA-2*KA*XA)/XA^2
2399      LX=XC-XB: LY=YC-YB: AB=(KB*LX+KC*LX-2*LY)/LX^3: BB=(3*LY-KC*LX-2*KB*LX
)/LX^2
2407 REM
2408 REM      Follow path for each time step H until zero velocity is reached
2409 REM
2410      A$=INKEY$: IF A$="" THEN 2418
2412      A$=RIGHT$(A$,1)
2414      IF A$="M" THEN H=.001
2416      IF A$="K" THEN H=-.001
2417      IF A$="P" THEN 2499
2418      D1=D2: D2=D2+H
2419      IF Z=1 AND D2-D1<0 THEN Z=-1: XMP=D1: YMP=R2: SLP=SL: KAVP=(YC-YB)/(X
C-XB): GOTO 2220
2420      IF Z=-1 AND D2-D1>0 THEN Z=1: XMN=D1: YMN=R2: SLN=SL: KAVN=(YC-YB)/(X
C-XB): GOTO 2220
2430 REM
2431 REM      Determine resisting force for particular deflection
2432 REM
2433      X=D2-XM
2435      IF X*Z<XA*Z THEN Y=AA*X^3+BA*X^2+KA*X: SL=3*AA*X^2+2*BA*X+KA
2436      IF X*Z>XA*Z AND X<XB*Z, THEN Y=YA+KB*(X-XA): SL=KB
2438      IF X*Z>XB*Z AND X<XC*Z, THEN X0=X-XB: Y=YB+AB*X0^3+BB*X0^2+KB*X0: SL
=3*AB*X0^2+2*BB*X0+KB
2440      IF X*Z>XC*Z THEN Y=YC+KC*(X-XC): SL=KC
2445      IF (Y+YM)*Z>((X+XM)*KC+B)*Z THEN Y=-YM+(X+XM)*KC+B
2450      R2=Y+YM
2460      U=160+D2*2500: V=100-R2*50/BP: LINE -(U,V),1 'Plot segment'
2465      GOTO 2410
2499 RETURN
2500 REM
2501 REM      This subroutine requests from the user information to construct
2502 REM      a hysteretic relation. The force-deflection relation is expressed
2503 REM      in terms of the base shear/weight and the top-level deflect/height.
2504 REM
2505 REM
2514 CLS: KEY OFF: SCREEN 1,0,0: COLOR 1,0
2515 LINE (10,10)-(310,170),3,8: LINE (10,10)-(310,100),3: LINE (160,10)-(160,
170),3
2518 LOCATE 3,3: PRINT "Base Shear/Weight":LOCATE 23,8: PRINT "Top-Level Deflec
tion/Height"
2519 LOCATE 1,1: PRINT "Specify strength envelopes"
2520 LINE (160,100)-(160,50),2: LINE (160,50)-(260,35),2: CIRCLE (160,50),5,3:
PAINT (160,50),2,3
2521 LOCATE 7,10: INPUT;"Force";BP: LOCATE 5,23: INPUT;"Slope";KCP
2530 LINE (160,100)-(160,140),2: LINE (160,140)-(60,150),2: CIRCLE (160,140),5,
3: PAINT (160,140),2,3
2532 LOCATE 17,22: INPUT;"Force";BN: LOCATE 18,7: INPUT;"Slope";KCN
2535      IF BN>0 THEN BN=-BN

```

```

(160,170),3
2544 LOCATE 3,3: PRINT "Base Shear/Weight":LOCATE 23,8: PRINT "Top-Level Deflec
tion/Height"
2550 LOCATE 1,1: PRINT "Specify yield deflections"
2560 LINE (160,50)-(260,50-.04*KCP*50/BP),1
2570 LINE (160,100)-(185,(100-(.01*KCP+BP)*50/BP)),2: LINE -(185,100),3
2580 LOCATE 11,24: INPUT;"Defl.":XYP
2590 LINE (160,100-BN*50/BP)-(60,100-BN*50/BP+.04*KCN*50/BP),1
2592 LINE (160,100)-(135,(100-(-.01*KCN+BN)*50/BP)),2: LINE -(135,100),3
2593 LOCATE 15,9: INPUT;"Defl.":XYN
2594 IF XYN>0 THEN XYN=-XYN
2600 CLS: LINE (10,10)-(310,170),3,B: LINE (10,100)-(310,100),3: LINE (160,10)-
(160,170),3
2610 LOCATE 3,3: PRINT "Base Shear/Weight":LOCATE 23,8: PRINT "Top-Level Deflec
tion/Height"
2612 LOCATE 1,1: PRINT "Specify unloading slopes"
2630 LINE (160,100)-(160+XYP*2500,(100-(XYP*KCP+BP)*50/BP)),1: LINE -(235,(50-.
03*KCP*50/BP)),1
2635 LINE -((235-XYP*2500),100),2: LOCATE 8,28: INPUT;"Slope":KAP
2640 LINE (160,100)-(160+XYN*2500,(100-(XYN*KCN+BN)*50/BP)),1: LINE -(85,(100-(
-.03*KCN+BN)*50/BP)),1
2645 LINE -((85-XYN*2500),100),2: LOCATE 17,6: INPUT;"Slope":KAN
2700 CLS: LINE (10,10)-(310,170),3,B: LINE (10,100)-(310,100),3: LINE (160,10)-
(160,170),3
2710 LOCATE 3,3: PRINT "Base Shear/Weight":LOCATE 23,8: PRINT "Top-Level Deflec
tion/Height"
2712 LOCATE 1,1: PRINT "Specify reversal slopes"
2730 LINE (160,100)-(160+XYP*2500,(100-(XYP*KCP+BP)*50/BP)),1: LINE -(235,(50-.
03*KCP*50/BP)),1: LINE -((235-(BP+.03*KCP)/KAP*2500),100),1
2735 LINE -(160,120),2: LOCATE 14,25: INPUT;"Slope":KEN
2740 LINE (160,100)-(160+XYN*2500,(100-(XYN*KCN+BN)*50/BP)),1: LINE -(85,(100-(
-.03*KCN+BN)*50/BP)),1: LINE -((85-(BN-.03*KCN)/KAN*2500),100),1
2745 LINE -(160,80),2: LOCATE 12,11: INPUT;"Slope":KBP
2800 CLS: LINE (10,10)-(310,170),3,B: LINE (10,100)-(310,100),3: LINE (160,10)-
(160,170),3
2810 LOCATE 3,3: PRINT "Base Shear/Weight":LOCATE 23,8: PRINT "Top-Level Deflec
tion/Height"
2812 LOCATE 1,1: PRINT "Verify"
2820 X1=(BP+.03*KCP)/KAP
2830 LINE (160,100)-(160+XYP*2500,(100-(XYP*KCP+BP)*50/BP)),2: LINE -(235,(50-.
03*KCP*50/BP)),2: LINE -((235-X1*2500),100),2: LINE -(160,(100+(.03-X1)*KBN*50/B
P)),2
2835 X2=(BN-.03*KCN)/KAN
2840 LINE (160,100)-(160+XYN*2500,(100-(XYN*KCN+BN)*50/BP)),2: LINE -(85,(100-(
-.03*KCN+BN)*50/BP)),2: LINE -((85-X2*2500),100),2: LINE -(160,(100+(-.03-X2)*KB
P*50/BP)),2
2850 H=.002: DBLP=8*XYP: DELN=8*XYN
2860 LOCATE 1,1: INPUT "Do you want to check hysteresis";A$: IF A$="no" OR A$="N
O" THEN 23
2870 GOTO 22
2900 FOR I=1 TO 1000: NEXT I: RETURN
3000 REM
3030 REM This subroutine opens a particular file to read a desired
3031 REM earthquake motion.
3032 REM
3035 REM
3036 REM Store alphanumeric labels in arrays
3037 REM
3040 A$(1)="Imperial Valley Earthquake - May 18 1940 - El Centro - NS":
B$(1)="CENTRO"
3041 A$(2)="San Fernando Earthquake - Feb 9 1971 - Pacoima Dam - S16E":
B$(2)="PACOMA"
3042 A$(3)="San Fernando Earthquake - Feb 9 1971 - Castaic Old Ridge Route - N21
E":B$(3)="CASTAC"
3043 A$(4)="San Fernando Earthquake - Feb 9 1971 - 3710 Wilshire Blvd - 1055-23

```

```

3044 A$(5)="Parkfield Earthquake - June 27 1966 - Temblor - S25W":
      B$(5)="TEMBLO"
3045 A$(6)="Kern Co. Earthquake - July 21, 1952 - Santa Barbara Courthouse - S48
E ":B$(6)="SANBAR"
3046 A$(7)="Parkfield Earthquake - June 27 1966 - Cholame, Shandon - N85E":
      B$(7)="CHOLAM"
3047 A$(8)="Miyagi Earthquake":      B$(8)="MIYA"
3048 A$(9)="Tokachi-Oki Earthquake":  B$(9)="TOKI"
3085 CLS: SCREEN 0,1,0: WIDTH 80: COLOR 15,1
3095 CLS: LOCATE 1,1: PRINT "Select a motion": PRINT ""
3096 PRINT "Scan options using up and down arrows": PRINT "Make selection with
right arrow": PRINT ""
3100 COLOR 8,1: FOR I=1 TO 9: PRINT A$(I): PRINT " ": NEXT I
3105 J=0: K=0: LOCATE 6,1
3110 A$=INKEY$: IF A$="" THEN 3110
3112 A$=RIGHT$(A$,1)
3114 IF A$="H" THEN J=J-1
3115 IF A$="P" THEN J=J+1
3116 IF J<1 OR J>9, THEN 3110
3117 IF A$="M" THEN 3122
3118 IF K=0 THEN 3120
3119 COLOR 8,1,0: LOCATE Y1,1: PRINT A$(K)
3120 COLOR 2,1,0: Y=2*J+4: LOCATE Y,1: Y1=Y: K=J: PRINT A$(J): GOTO 3110
3122 C$="B:"+B$(J)+".DAT"
3124 OPEN "I",#1,C$: INPUT #1,A$: INPUT #1, AMAX1,TSTEP,DUR
3128 CLS: COLOR 2,1,0: PRINT "Duration of record is ";DUR;" secnds": PRINT "In
put desired duration":INPUT DUR: N=DUR/TSTEP
3129 PRINT " ": PRINT "Time scale factor is equal to 1.0": PRINT "Input desired
time scale factor": INPUT TSCALE
3135 PRINT " ": PRINT "Maximum recorded ground acceleration was ";AMAX1;"g": PRI
NT "Input desired maximum":INPUT AMAX
3137 INPUT #1, P4: P4=P4*AMAX/AMAX1
3140 RETURN
4000 REM
4010 REM This subroutine introduces the user to the program, reads
4011 REM the mass distribution and choice of deflected shape,
4012 REM and then computes the generalized mass terms,
4013 REM and fundamental mode participation factor.
4014 REM
4016 REM
4017 REM Introduce program to user
4018 REM
4020 CLS: SCREEN 0,1,0: COLOR 2,8: KEY OFF: WIDTH 40: LOCATE 4,6: PRINT "NONLIN
EAR SEISMIC ANALYSIS": LOCATE 6,9: PRINT "OF BUILDING SYSTEMS"
4021 LOCATE 12,14: PRINT "written by": LOCATE 14,11: PRINT "Daniel P. Abrams"
4022 LOCATE 16,8: PRINT "University of Illinois": LOCATE 17,9: PRINT "at Urbana
-Champaign": FOR I=1 TO 1000: NEXT I
4023 CLS: WIDTH 80: LOCATE 1,1: PRINT "This program computes nonlinear dynamic
response of building systems that may be characterized solely with their fundame
ntal mode of response.": PRINT ""
4024 PRINT "Required input information consists of:": PRINT ""
4025 PRINT " (a) mass distribution"
4026 PRINT " (b) form of lateral deflected shape"
4027 PRINT " (c) ratio of base-shear capacity to building weight"
4028 PRINT " (d) overall stiffness in terms of ratio of top-level deflection
to height:"
4029 PRINT " (e) selection of hysteresis formulation"
4030 PRINT " (f) selection of earthquake motion": PRINT ""
4031 PRINT "Output information consists of:":PRINT ""
4032 PRINT " (a) response histories of acceleration and lateral deflection"
4033 PRINT " (b) nonlinear force-deflection relation"
4035 PRINT " ": PRINT "Please follow along....."
4040 LOCATE 20,15: PRINT "Press right arrow to continue"
4042 A$=INKEY$: IF A$="" THEN 4042
4043 A$=RIGHT$(A$,1)

```



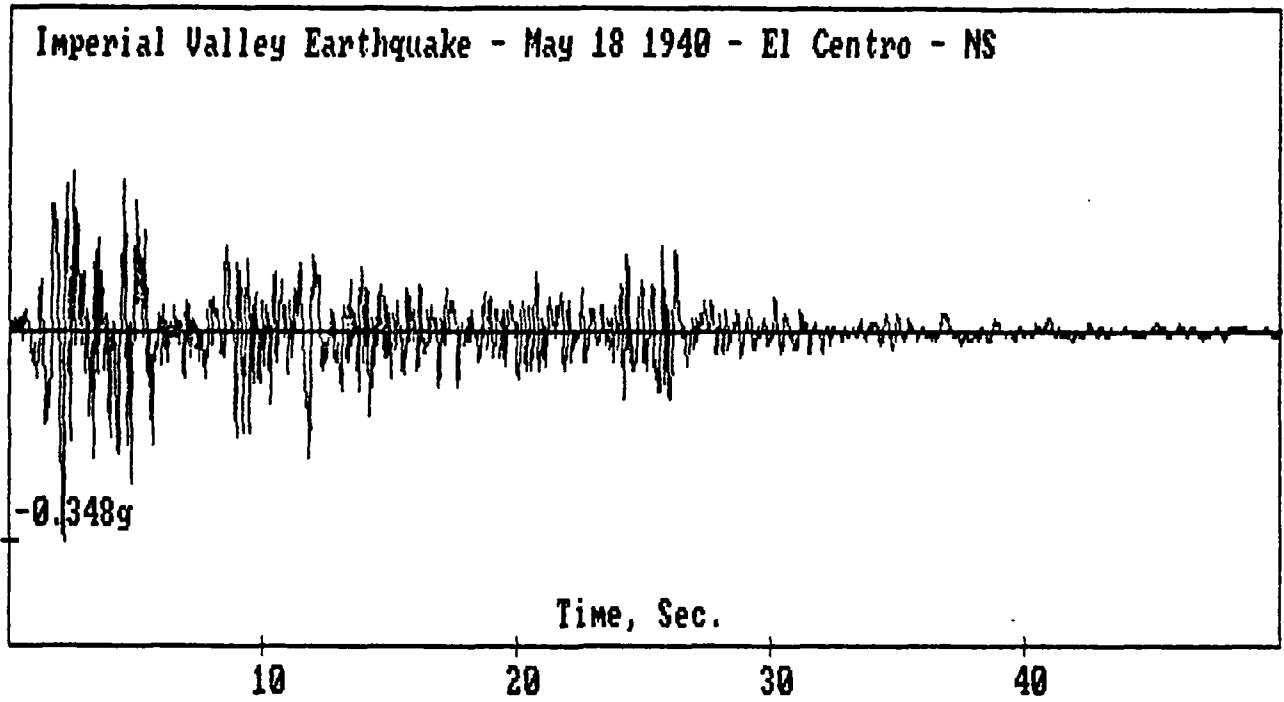
```
4230 A$=INKEY$: IF A$="" THEN 4240  
4231 A$=RIGHT$(A$,1): IF A$="M" THEN 4250  
4240 NEXT K  
4250 RETURN
```

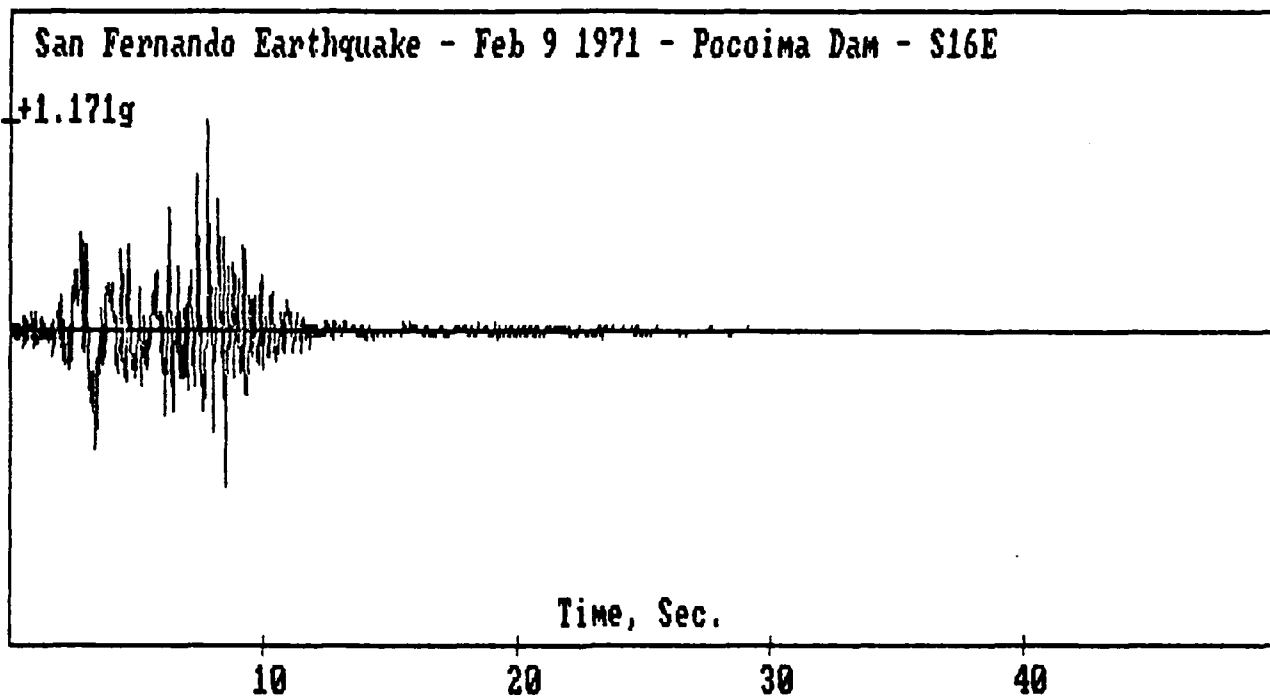
APPENDIX C EARTHQUAKE RECORDS

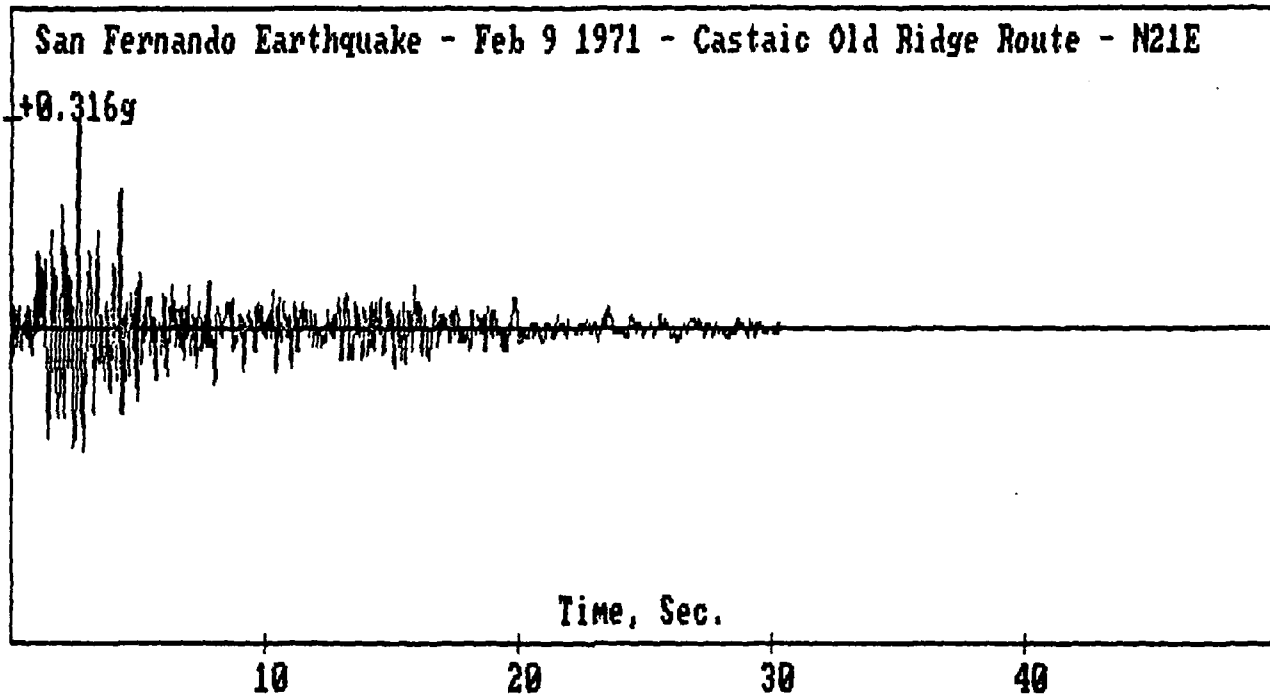
The following accelerograms have been stored on diskette, and may be retrieved easily using the menu provided by the program.

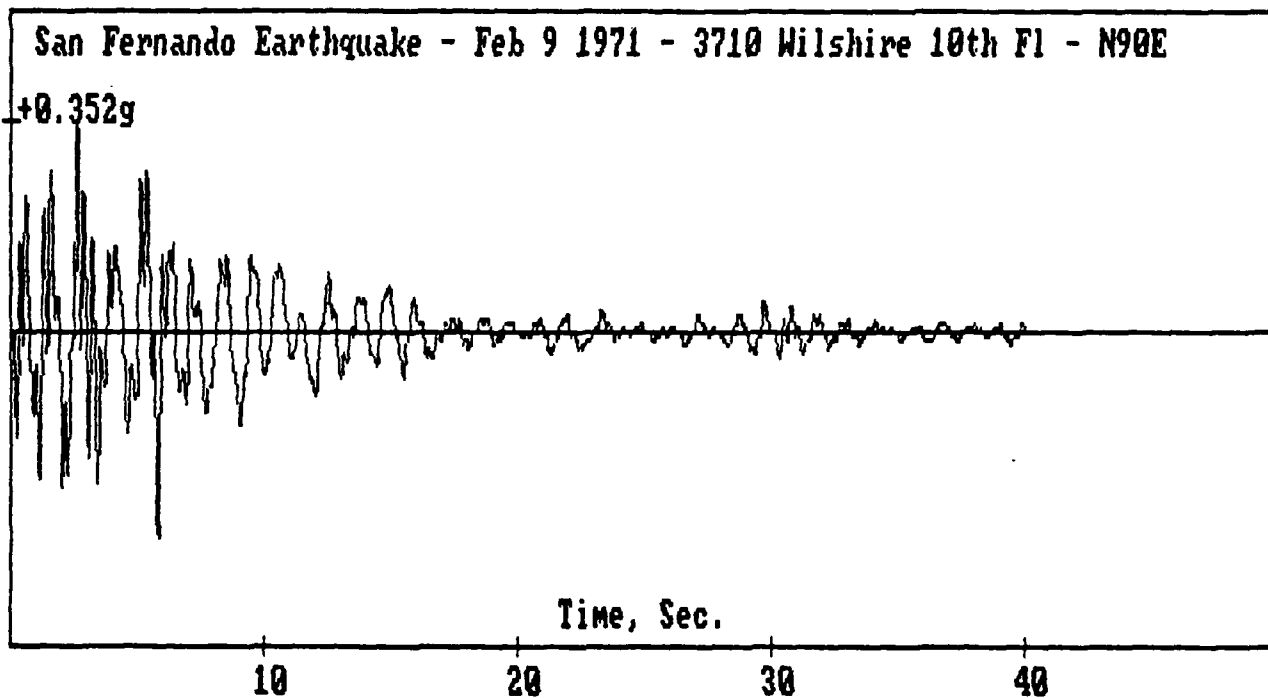
The motions were reformatted from USGS records. The effort of Mr. Art Schultz, former research assistant at the University of Illinois, is acknowledged for acquiring the USGS records.

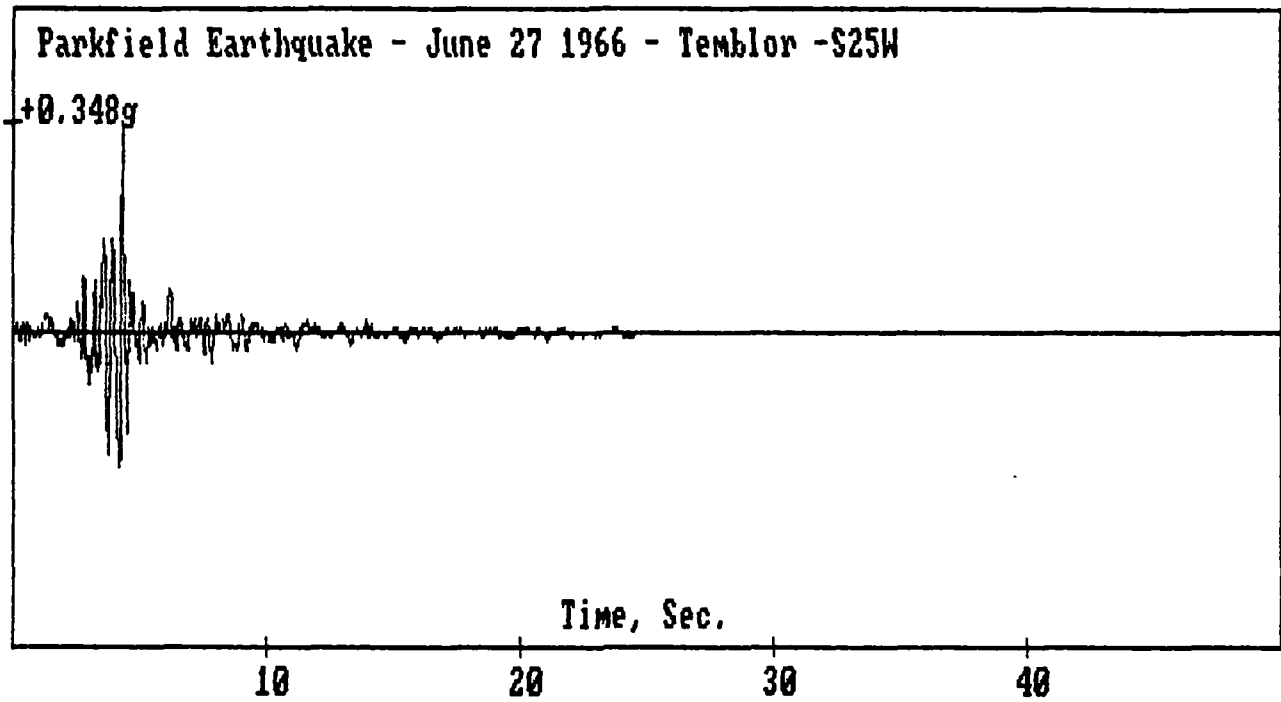
In addition, a listing of a BASIC computer program, "BMOTION", is provided which was written to read the USGS records and reformat for use with the program.

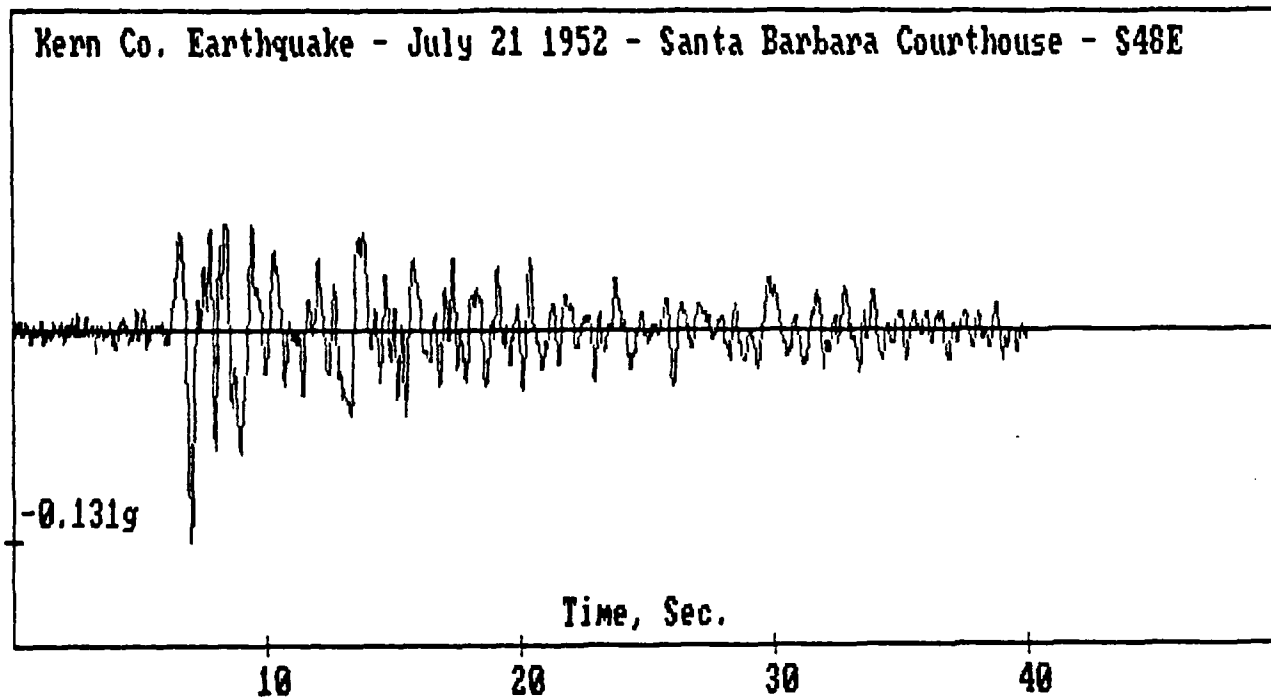


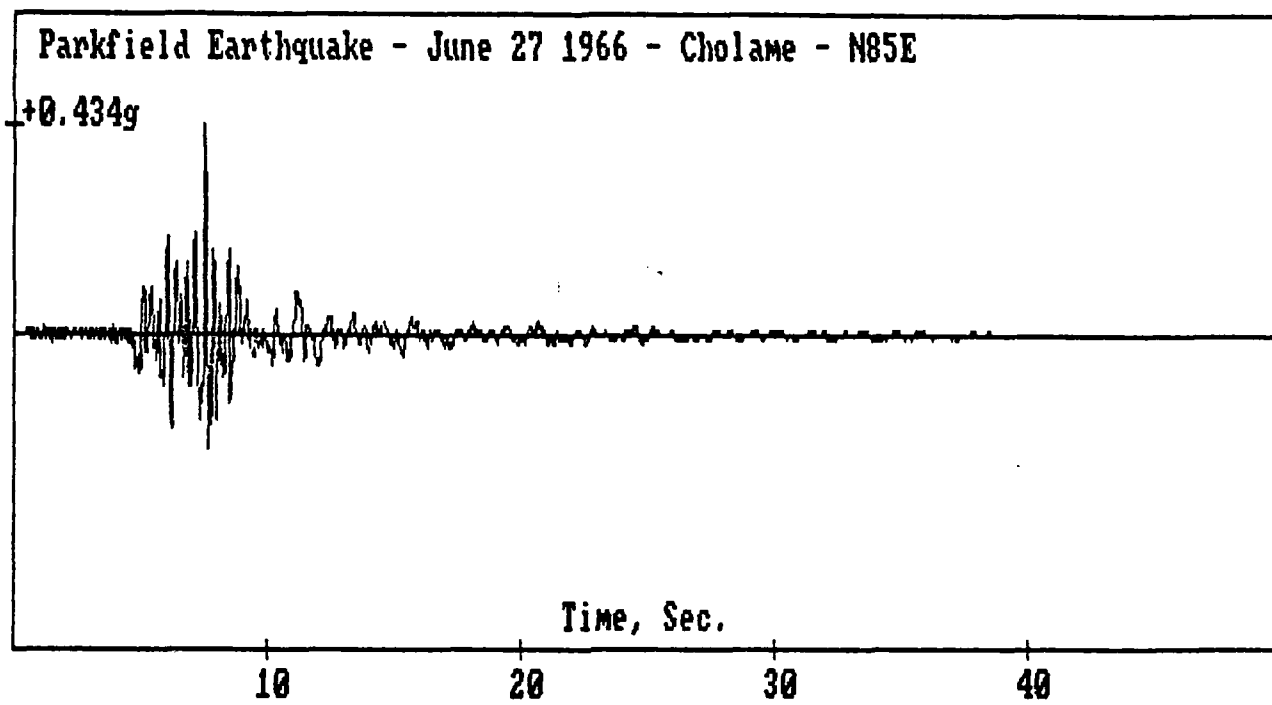


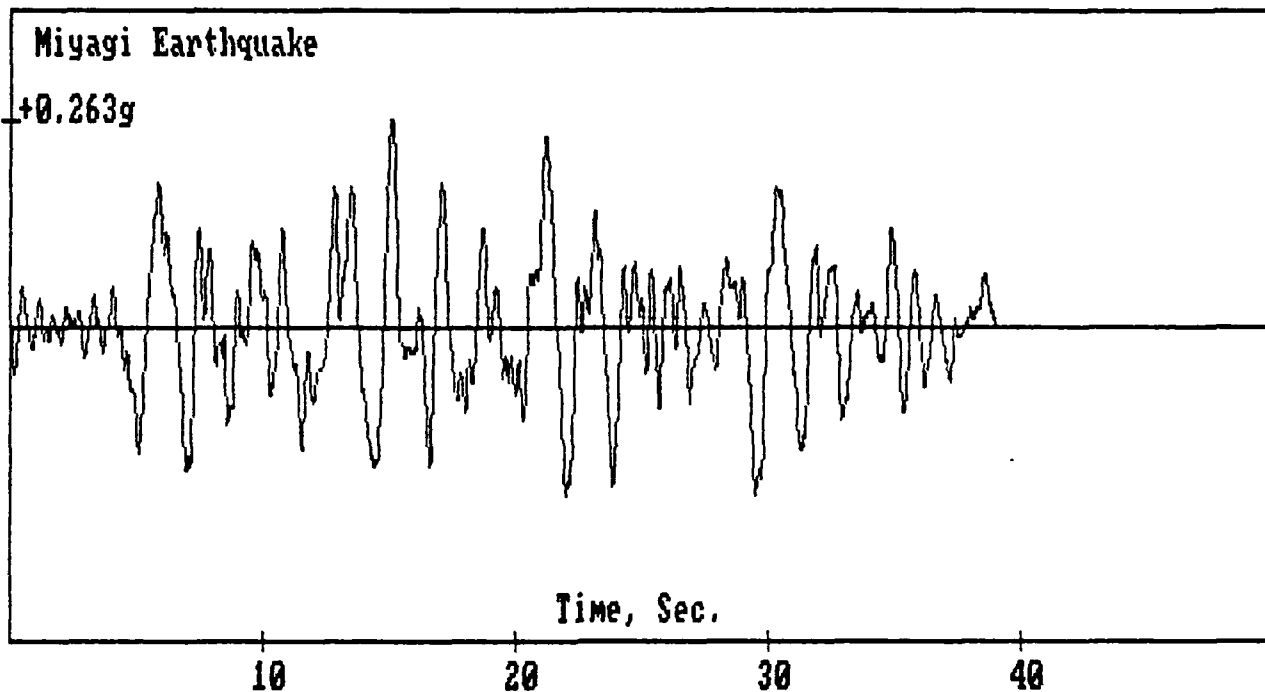


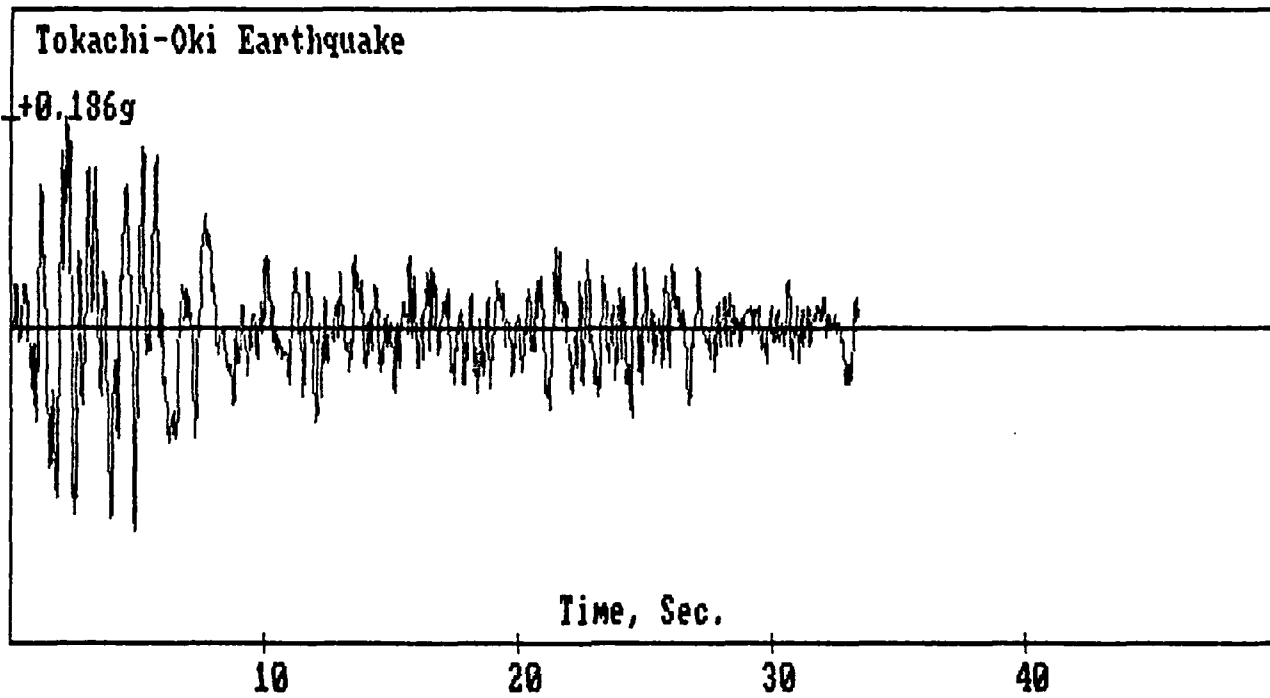












```

1  REM  THIS PROGRAM READS AN EARTHQUAKE FILE FROM DISK A IN USGS FORMAT
2  REM  AND PRINTS IT ON ANOTHER FILE ON DISK B IN A SIMPLER FORMAT.
3  REM  HEADER INFORMATION IS AS FOLLOWS:
4  REM    LABEL
5  REM    AMAX, TSTEP, DUR.
6  REM  ACCELERATION DATA ARE NORMALIZED WITH RESPECT TO G, AND ARE LISTED
7  REM  IN GROUPS OF FIVE PER LINE.
8  DIM P(4000)
9  PRINT "Place source record in drive B": PRINT "Name of earthquake?": INP
UT M$
10  N$="B:"+M$+".DAT": OPEN "I",#1,N$
15  PRINT "Specify duration of earthquake in seconds": INPUT N: N=N*50
20  PRINT "Input number of header lines to skip": INPUT R
22  FOR I=1 TO R: INPUT #1, A$: NEXT I
24  PRINT "Input STOP if last line of header information has been read"
25  INPUT #1, A$: PRINT A$: INPUT B$: IF B$="STOP" THEN 30
26  GOTO 25
28  REM  INPUT FILE FROM DISK B
30  FOR J=1 TO N/5: I=5*(J-1): INPUT #1,P(I+1),P(I+2),P(I+3),P(I+4),P(I+5)
40  NEXT J
60  CLOSE #1
65  REM  PRINT HEADER INFORMATION ON DISK A
66  PRINT "Place formatted disk in drive A for copy"
70  N$="A:"+M$+".DAT": OPEN "O",#1,N$
80  PRINT "Input label": INPUT A$: PRINT #1, A$
82  G=980.665: TSTEP=.02: DUR=N*TSTEP
85  PRINT "Input AMAX in cm/s/s": INPUT AMAX: AMAX=AMAX/G
90  PRINT #1, AMAX, TSTEP, DUR
101 REM  PRINT RECORD TO DISK B
110  FOR J=1 TO N/5: I=5*(J-1): PRINT#1,USING " +#.##### ";P(I+1)/G,P(I+2)
/G,P(I+3)/G,P(I+4)/G,P(I+5)/G: NEXT J: CLOSE #1
115 REM  VERIFY COPY PROCEDURE
130  PRINT "Do you wish to verify copy?": INPUT A$: IF A$="NO" OR A$="no" THE
N 200
132  OPEN "I",#1,N$: INPUT #1, A$
133  INPUT #1, AMAX, TSTEP, DUR: N=DUR/TSTEP
134  FOR J=1 TO N/5: I=5*(J-1): INPUT #1, P(I+1),P(I+2),P(I+3),P(I+4),P(I+5)
135  NEXT J: CLOSE #1
136 REM  PRINT FILE ON SCREEN
140  PRINT "Do you wish to see data file?": INPUT B$: IF B$="no" OR B$="NO" T
HEN 149
145  PRINT A$: PRINT AMAX, TSTEP, DUR: FOR J=1 TO N/5: I=5*(J-1): PRINT USING "
+#.##### ";P(I+1),P(I+2),P(I+3),P(I+4),P(I+5): NEXT J
148 REM  PLOT WAVEFORM ON SCREEN
149  PRINT "Do you wish to plot ground motion?": INPUT B$: IF B$="no" OR B$="
NO" THEN 200
180  CLS: SCREEN 2,0,0: S=2: KEY OFF
185  LINE (10*S,3)-(310*S,160),1,B: LINE (310*S,80)-(10*S,80),1
186  LOCATE 2,2*S: PRINT A$
188  FOR I=0 TO 5: X=(10+I*60)*S: Y=I*10: LINE (X,158)-(X,162),1: LOCATE 22,(
X/8-1): PRINT Y: NEXT I
190  LOCATE 23,16*S: PRINT "Time, Seconds"
192  Y=(80-60*AMAX/(ABS(AMAX))): LINE (8*S,Y)-(12*S,Y),1: LOCATE Y/3,2*S: PR
INT AMAX: LINE -(10*S,80),0
195  FOR I=1 TO 2500: Y=80-P(I)/(ABS(AMAX))*60: X=I*300*S/2500+10*S: LINE -(X
,Y),1: NEXT I
196  FOR I=1 TO 10000: NEXT I

```

END

FILMED

2-86

DTIC